



# New insights into the phylogeny and skull evolution of stegosaurian dinosaurs: An extraordinary cranium from the European Late Jurassic (Dinosauria: Stegosauria)

Sergio Sánchez-Fenollosa<sup>1</sup>, Alberto Cobos<sup>1</sup>

<sup>1</sup> *Fundación Conjunto Paleontológico de Teruel-Dinópolis / Museo Aragonés de Paleontología, Av. Sagunto S/N, 44002 Teruel, Teruel, Spain*

<https://zoobank.org/2B64FEC4-268A-4840-9FD4-E2F8C42F3475>

Corresponding author: Sergio Sánchez-Fenollosa (sfenollosa@fundaciondinopolis.org)

Academic editor Uwe Fritz

Received 18 January 2025

Accepted 15 April 2025

Published 26 May 2025

**Citation:** Sánchez-Fenollosa S, Cobos A (2025) New insights into the phylogeny and skull evolution of stegosaurian dinosaurs: An extraordinary cranium from the European Late Jurassic (Dinosauria: Stegosauria). *Vertebrate Zoology* 75: 165–189. <https://doi.org/10.3897/vz.75.e146618>

## Abstract

Stegosauria is an iconic clade of thyreophoran dinosaurs mainly characterized by two parasagittal rows of osteoderms that extend from the neck to the end of the tail. The fossil record of stegosaurian cranial material is remarkably fragmentary and scarce. This study describes the most complete stegosaurian skull from Europe and proposes a new hypothesis for the phylogenetic relationships of stegosaurs. This new cranial material was recovered from beds of the Villar del Arzobispo Formation (Upper Jurassic, Teruel, Spain) and is confidently referred to *Dacentrurus armatus*. It provides valuable insights into the anatomy of this species and enhances the understanding of skull evolution in stegosaurs. Furthermore, the diagnosis of *D. armatus* is updated with the identification of a new autapomorphy. Stegosaurian phylogenetic nomenclature is also revised. Maximum Parsimony has been applied to analyse a new stegosaurian data matrix. Phylogenetic analyses suggest that Stegosauria is divided into two major clades: Huayangosauridae and Stegosauridae. These analyses support *Isaberrysaura mollensis* as a stegosaur and place it within Huayangosauridae, a clade that also includes several Jurassic stegosaurs from Asia. For the first time, *Mongolostegus exspectabilis* is included in a phylogenetic analysis, the results of which suggests that a lineage of huayangosaurids or early-diverging stegosaurids persisted in Asia until at least the late Early Cretaceous. The new tree topologies challenge the synonymization of the genera *Stegosaurus* and *Wuerhosaurus*. Moreover, it is concluded that a taxonomic re-evaluation of Early Cretaceous Chinese stegosaurs is necessary. *Alcovasaurus longispinus* and *Kentrosaurus aethiopicus* are recovered as dacentrurines.

## Keywords

Character evolution, Maximum Parsimony, Mesozoic, morphological phylogenetics, Neostegosauria, phylogenetic nomenclature, systematics, Thyreophora

## Introduction

The name Stegosauria was erected almost 150 years ago (Marsh 1877) and the first stegosaur, *Dacentrurus armatus* Owen, 1875, was described two years earlier (Owen 1875). Stegosauria is a small clade of thyreophoran dinosaurs that includes some iconic and recognizable members, such as the genus *Stegosaurus* Marsh, 1877 (e.g., Galton and Upchurch 2004; Maidment et al. 2008). They were quadrupedal herbivores mainly characterized by

two parasagittal rows of osteoderms (plates and spines) that extend from the neck to the tail end (e.g., Sereno 1986; Galton and Upchurch 2004; Maidment et al. 2008). The stegosaurs are known from, at least, Middle Jurassic to possibly the Late Cretaceous in sediments from almost worldwide (Galton and Upchurch 2004; Maidment et al. 2008, 2020), but mostly represented by single partial skeletons (Raven and Maidment 2017).

The stegosaurian cranial material fossil record is remarkably fragmentary and scarce. Nearly half of the current valid taxa of stegosaurs do not preserve cranial material (e.g., Galton 2016; Galton and Carpenter 2016; Tumanova and Alifanov 2018; Maidment et al. 2020; Dai et al. 2022; Jia et al. 2024; Li et al. 2024a; Zafaty et al. 2024). Only three taxa preserve a significant part of their skull: *Huayangosaurus taibaii* Dong, Tang & Zhou, 1982, *Hesperosaurus mjosi* Carpenter, Miles & Cloward, 2001, and *Stegosaurus stenops* Marsh, 1887 (Sereno and Dong 1992; Carpenter et al. 2001; Galton and Upchurch 2004). This represents a critical problem for understanding the evolutionary relationship of stegosaurs, as well as their ecological role. Regarding the European record, only two stegosaurian specimens classified as *D. armatus* (Sánchez-Fenollosa et al. 2025), preserve cranial elements (Mateus et al. 2009; Costa and Mateus 2019).

The first attempts to reconstruct the evolutionary history of stegosaurs using cladistics date back to the early 1990s (Sereno and Dong 1992). However, this pioneering analysis was highly limited, including only 22 characters and grouping most stegosaurs (except *H. taibaii* and *D. armatus*) into a single supraspecific OTU labelled 'other stegosaurs'. Carpenter et al. (2001) produced a preliminary phylogeny of Stegosauria, which, for the first time, treated many stegosaurian genera as discrete OTUs. However, this analysis relied on just 12 characters. A more comprehensive phylogenetic study was conducted by Galton and Upchurch (2004), incorporating 11 stegosaurian taxa and 55 characters. Despite this improvement, the resolution of the results was low. Later, Escaso et al. (2007a) expanded and modified this data matrix for their own phylogenetic analysis of Stegosauria.

A major step forward came with Maidment et al. (2008), who produced a stegosaurian phylogeny based on first-hand observations. Their analysis included 11 stegosaurian taxa and 85 characters, building upon a preliminary version presented by Maidment et al. (2006). This phylogeny was slightly updated by Mateus et al. (2009) and Maidment (2010). The most significant update occurred in 2017, when this data matrix was converted to treat continuous data as such, added several new characters, and investigated applying new search algorithms (Raven and Maidment 2017). The resulting data matrix has been the basis for subsequent phylogenetic analyses (e.g., Maidment et al. 2020; Dai et al. 2022; Jia et al. 2024; Li et al. 2024a). However, some issues and errors present in the original data matrix have persisted in these later studies, conditioning the results obtained and limiting alternative hypotheses.

In the present study, we describe the most complete stegosaurian skull from Europe and we provide a new phylogeny. The aims of this study are to: (1) provide a detailed description of this extraordinary fossil; (2) assign it taxonomically; (3) revise the stegosaurian phylogenetic nomenclature; (4) build a new morphological data matrix; (5) infer the evolutionary relationships of stegosaurs, and (6) discuss the taxonomic and evolutionary implications of our results.

## Geographical and geological setting

The fossils studied here come from the Están de Colón (RD-34) site, which is in the municipality of Riodeva (province of Teruel, Aragón, Spain) (Fig. 1A, B).

Geologically, RD-34 is included in the South-Iberian Basin (Fig. 1A, B). The South-Iberian Basin presents a NW–SE orientation and is part of the Mesozoic Iberian Extensional System (e.g., Campos-Soto et al. 2021). This basin was developed in eastern Iberia during the late Oxfordian–middle Albian and inverted during the Cenozoic Alpine Orogeny (e.g., Mas et al. 2004; Campos-Soto et al. 2019, 2021).

RD-34 is located in the upper half of the Villar del Arzobispo Formation (upper Kimmeridgian–Tithonian sensu Campos-Soto et al. 2017, 2019) section in the Riodeva area (Campos-Soto et al. 2019) (Fig. 1C). It is a detrital-carbonate lithostratigraphic unit formed by sandstone and clay levels with intercalations of limestone and marls (Mas et al. 1984). This unit comprises two informal parts (Campos-Soto et al. 2019): (1) an essentially carbonate lower part (CLP, upper Kimmeridgian) and an essentially siliciclastic upper part (SUP, upper Kimmeridgian–Tithonian). Deposits of the SUP have been interpreted as deposited in a coastal and alluvial plain (Campos-Soto et al. 2019, 2021). Concretely, the fossils studied here were located in a sandstone layer.

The Villar del Arzobispo Formation overlies the oncologic limestone unit Higuieruelas Formation (Kimmeridgian sensu Campos-Soto et al. 2016; Pacios et al. 2018).

## Material and methods

### Site description and fossils studied

Están de Colón (RD-34) fossil site was discovered in 2004 and partially excavated in 2006 and 2007. This site was first mentioned at a conference in 2008 (Cobos et al. 2008). RD-34 was found in a crop field with an area of approximately 24 m<sup>2</sup>. During the two excavation campaigns, around 200 elements were recovered. The freshwater bivalve *Margaritifera cf. valdensis* Mantell, 1844 was reported at this site (Delvene et al. 2013). The preliminary study of this huge fossil site reveals that most of these fossils correspond to at least two stegosaurian specimens at different ontogenetic stages. In addition to the stegosaurs, RD-34 also yielded several theropod, sauropod, ornithomorph, and osteichthyan fossils. The fossils studied here comprise a partial cranium (MAP-9029) and a mid cervical vertebra (MAP-9030). MAP-9029 and MAP-9030 are considered to belong to the same specimen because they came from the same layer, they were found associated (distance between them around 5 cm), and the size and features of the pieces are consistent. Additional postcranial fossils of this specimen were recovered; however, their systematic study is beyond the scope of this paper and some of them are still unprepared.

The studied fossils are deposited in the Museo Aragonés de Paleontología (Teruel, Spain).

## Phylogenetic nomenclature

The requirements of the International Code of Phylogenetic Nomenclature (PhyloCode) were met and its recommendations followed to formally establish the clade names. For each clade the following information was included: clade name, designation (new or converted), registration number, phylogenetic definition, reference phylogeny, hypothesized composition, and comments. Furthermore, an etymology section was also added in the case of new clade names. All clade names were registered in the Regnum repository ([www.phyloregnum.org](http://www.phyloregnum.org)).

## Data matrix building

The data matrices (Files S2 and S3) were built using the MESQUITE v.3.81 software (Maddison and Maddison 2023).

The character list was primarily based on the stegosaurian-focused analyses by Sereno and Dong (1992), Galton and Upchurch (2004), Maidment et al. (2008), and Raven and Maidment (2017), with additional input from broader studies that focus on ornithischians, thyrocephorans, and ankylosaurs (Sereno 1999; Butler et al. 2008; Soto-Acuña et al. 2021; Raven et al. 2023). These datasets were thoroughly evaluated, resulting in the exclusion or modification of several characters as required (File S1 [1.4]). Furthermore, 20 new characters were added (File S1 [1.4]). The final character list contains 115 characters:

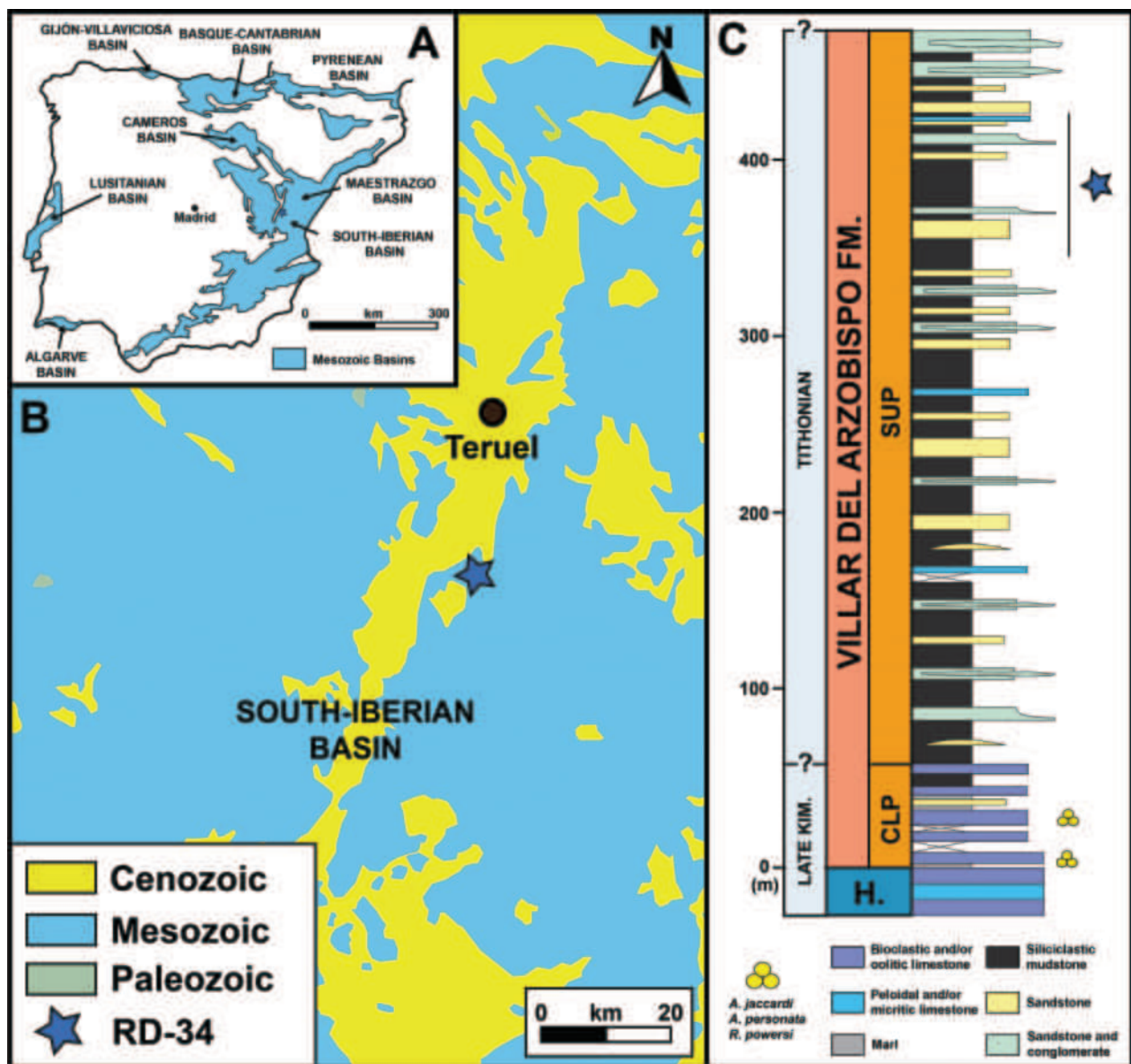


**Figure 1. A, B** location and geological setting of the Están de Colón (RD-34) fossil site in Riodeva (Teruel, Spain). **C** stratigraphic section of the Villar del Arzobispo Formation in the Riodeva area. Cartography and stratigraphic section modified from Campos-Soto et al. (2019).

**Table 1.** Operational Taxonomic Unit list and source of scoring. See File S1 [1.3] for more information about the specimens examined first-hand and the geographic and chronostratigraphic distribution of each OTU.

	OTU	Source of scoring
	<i>Lesothosaurus diagnosticus</i>	Thulborn (1972), Galton (1978), Sereno (1991), Butler (2005), Porro et al. (2015), Baron et al. (2017), pers. obs.
<b>Early-diverging thyreophorans</b>	<i>Scutellosaurus lawleri</i>	Colbert (1981), Rosenbaum and Padian (2000), Breeden and Rowe (2020), Breeden et al. (2021)
	<i>Emausaurus ernsti</i>	Haubold (1990), Norman et al. (2004)
	<i>Yuxisaurus kopchicki</i>	Yao et al. (2022)
	<i>Scelidosaurus harrisonii</i>	Norman (2020a, 2020b, 2020c, 2021), pers. obs.
<b>Ankylosaurs</b>	<i>Europelta carbonensis</i>	Kirkland et al. (2013), pers. obs.
	<i>Euoplocephalus tutus</i>	Vickaryous and Russell (2003), Arbour and Currie (2013)
	<i>Ankylosaurus magniventris</i>	Carpenter (2004), Arbour and Mallon (2017)
<b>Stegosaurs</b>	<i>Isaberrysaura mollensis</i>	Salgado et al. (2017)
	<i>Huayangosaurus taibaii</i>	Zhou (1984), Sereno and Dong (1992), Galton and Upchurch (2004), Peng et al. (2005), Maidment et al. (2006), Li et al. (2024a)
	<i>Bashanosaurus primitivus</i>	Dai et al. (2022)
	<i>Baiyinosaurus baojiensis</i>	Li et al. (2024b)
	<i>Gigantospinosaurus sichuanensis</i>	Peng (2005), Maidment et al. (2008), Hao et al. (2018), Li et al. (2024a)
	<i>Chungkingosaurus jiangbeiensis</i>	Dong et al. (1983), Dong (1990), Galton and Upchurch (2004), Maidment and Wei (2006), Li et al. (2024a)
	<i>Mongolostegus exspectabilis</i>	Tumanova and Alifanov (2018)
	<i>Tuojiangosaurus multispinus</i>	Dong et al. (1977, 1983), Galton and Upchurch (2004), Maidment and Wei (2006), Li et al. (2024a)
	<i>Paranthodon africanus</i>	Galton and Coombs (1981), Raven and Maidment (2018), pers. obs.
	<i>Loricatosaurus priscus</i>	Galton (1985, 1990, 2016), pers. obs.
	<i>Hesperosaurus mjosi</i>	Carpenter et al. (2001), Galton and Upchurch (2004), Siber and Mœckli (2009), Bignon-Bruyat et al. (2010), Maidment et al. (2018)
	<i>Stegosaurus stenops</i>	Gilmore (1914), Ostrom and McIntosh (1966), Galton and Upchurch (2004), Escaso et al. (2007a), Maidment et al. (2015), pers. obs.
	<i>Jiangjunosaurus junggarensis</i>	Jia et al. (2007), Li et al. (2024a)
	<i>Wuerhosaurus homheni</i>	Dong (1973, 1990, 1993), Maidment et al. (2008), Li et al. (2024a)
	<i>Yanbeilong ultimus</i>	Jia et al. (2024)
	<i>Alcovasaurus longispinus</i>	Gilmore (1914), Galton and Carpenter (2016)
	<i>Kentrosaurus aethiopicus</i>	Hennig (1915a, 1916, 1925), Galton (1982, 1988), Galton and Upchurch (2004), Mallison (2010), Pereda-Suberbiola et al. (2013), pers. obs.
	<i>Thyreosaurus atlasticus</i>	Zafaty et al. (2024)
	<i>Adratiklit boulahfa</i>	Maidment et al. (2020), pers. obs.
	<i>Dacentrurus armatus</i>	Owen (1875), Nopcsa (1911b), Galton (1985; 1991), Casanovas-Cladellas et al. (1995), Escaso et al. (2007b), Mateus et al. (2009), Cobos et al. (2010), Escaso (2014), Costa and Mateus (2019), Sánchez-Fenollosa et al. (2022, 2025), pers. obs., this paper
	Qiketai stegosaur	Li et al. (2024a)
	Zhongpu stegosaur	Li et al. (2024c)

40 cranial, 27 axial, 38 appendicular, and 10 osteodermal (Files S1 [1.4], S2, S3). Character scorings were based on a strict bibliographic revision, photographs, 3D models, and, when possible, on first-hand observations (Table 1; File S1 [1.3]).

The unarmoured taxon *Lesothosaurus diagnosticus* Galton, 1978 was used as the outgroup. It is known from several specimens, some of which are highly complete, and was recovered as an early-diverging thyreophoran in a few analysis (Butler et al. 2008; Boyd 2015). However, these results are poorly supported by evidence and *L. diagnosticus* has recently been recovered as an early-diverging ornithischian, genasaurian, or neornithischian (e.g., Baron et al. 2017; Han et al. 2018; Dieudonné

et al. 2021; Fonseca et al. 2024). Following Baron et al. (2017), ‘*Stormbergia dangershoekei*’ Butler, 2005 is regarded as a subjective junior synonym of *L. diagnosticus*, and consequently, the latter taxon was coded (Thulborn 1972; Galton 1978; Sereno 1991; Butler 2005; Porro et al. 2015; Baron et al. 2017; pers. obs.). Four early-diverging thyreophoran taxa were included: *Scutellosaurus lawleri* Colbert, 1981 (Colbert 1981; Rosenbaum and Padian 2000; Breeden and Rowe 2020; Breeden et al. 2021), *Emausaurus ernsti* Haubold, 1990 (Haubold 1990; Norman et al. 2004), *Yuxisaurus kopchicki* Yao et al., 2022 (Yao et al. 2022), and *Scelidosaurus harrisonii* Owen, 1861 (Norman 2020a, 2020b, 2020c, 2021; pers. obs.), as well as three representative ankylosaurian taxa:

the nodosaurid (struthiosaurid sensu Raven et al. 2023) *Europelta carbonensis* Kirkland et al., 2013 (Kirkland et al. 2013; pers. obs.) and the ankylosaurids *Euoplocephalus tutus* Lambe, 1902 (Vickaryous and Russell 2003; Arbour and Currie 2013) and *Ankylosaurus magniventris* Brown, 1908 (Carpenter 2004; Arbour and Mallon 2017). Regarding stegosaurs, non-valid or dubious taxa (e.g., ‘*Craterosaurus pottonensis*’ Seeley, 1874, ‘*Chialingosaurus kuani*’ Young, 1959, ‘*Dravidosaurus blanfordi*’ Yadagiri & Ayyasami, 1979, ‘*Monkonosaurus lawulacus*’ Zhao in Dong, 1990) were excluded (Maidment and Wei 2006; Maidment et al. 2008) and 20 taxa were added: *Isaberrysaura mollensis* Salgado et al., 2017 (Salgado et al. 2017), *H. taibaii* (Zhou 1984; Sereno and Dong 1992; Galton and Upchurch 2004; Peng et al. 2005; Maidment et al. 2006; Li et al. 2024a), *Bashanosaurus primitivus* Dai et al., 2022 (Dai et al. 2022), *Baiyinosaurus baojiensis* Li et al., 2024b (Li et al. 2024b), *Gigantospinosaurus sichuanensis* Ouyang, 1992 (Peng 2005; Maidment et al. 2008; Hao et al. 2018; Li et al. 2024a), *Chungkingosaurus jiangbeiensis* Dong, Zhou & Chang, 1983 (Dong et al. 1983; Dong 1990; Galton and Upchurch 2004; Maidment and Wei 2006; Li et al. 2024a), *Mongolostegus exspectabilis* Tumanova & Alifanov, 2018 (Tumanova and Alifanov 2018), *Tuojiangosaurus multispinus* Dong, Li, Zhou & Chang, 1977 (Dong et al. 1977, 1983; Galton and Upchurch 2004; Maidment and Wei 2006; Li et al. 2024a), *Paranthodon africanus* Broom, 1910 (Galton and Coombs 1981; Raven and Maidment 2018; pers. obs.), *Loricatosaurus priscus* Nopcsa, 1911a (Galton 1985, 1990, 2016; pers. obs.), *He. mjosi* (Carpenter et al. 2001; Galton and Upchurch 2004; Siber and Möckli 2009; Biyon-Bruyat et al. 2010; Maidment et al. 2018), *S. stenops* (Gilmore 1914; Ostrom and McIntosh 1966; Galton and Upchurch 2004; Escaso et al. 2007a; Maidment et al. 2015; pers. obs.), *Jiangjunosaurus junggarensis* Jia, Foster, Xu & Clark, 2007 (Jia et al. 2007; Li et al. 2024a), *Wuerhosaurus homheni* Dong, 1973 (Dong 1973, 1990, 1993; Maidment et al. 2008; Li et al. 2024a), *Yanbeilong ultimus* Jia et al., 2024 (Jia et al. 2024), *Alcovasaurus longispinus* Gilmore, 1914 (Gilmore 1914; Galton and Carpenter 2016), *Kentrosaurus aethiopicus* Hennig, 1915a (Hennig 1915a, 1916, 1925; Galton 1982, 1988; Galton and Upchurch 2004; Mallison 2010; Pereda-Suberbiola et al. 2013; pers. obs.), *Thyreosaurus atlasicus* Zafaty et al., 2024 (Zafaty et al. 2024), *Adratiklit boulahfa* Maidment, Raven, Ouarhache & Barrett, 2020 (Maidment et al. 2020; pers. obs.), and *D. armatus* (Owen 1875; Nopcsa 1911b; Galton 1985, 1991; Casanovas-Cladellas et al. 1995; Escaso et al. 2007b; Mateus et al. 2009; Cobos et al. 2010; Escaso 2014; Costa and Mateus 2019; Sánchez-Fenollosa et al. 2022, 2025; pers. obs.; this paper). Moreover, the Qiketai stegosaur (Li et al. 2024a) and the Zhongpu stegosaur (Li et al. 2024c) were also included. Therefore, 30 Operational Taxonomic Units (OTUs) were considered (Table 1; Files S1 [1.3], S2).

To further test the taxonomic assignment of the stegosaurian specimen from RD-34 (Figs 2–4), it was also coded as an independent OTU (File S3).

## Phylogenetic analysis and time-scaling methodology

Maximum Parsimony (MP) analyses were conducted to infer the phylogenetic relationships of stegosaurs (File S1 [table S2]). The new data matrices (Files S2, S3) were analysed utilizing the TNT v.1.6 software (Goloboff and Morales 2023) and executing an initial search with ‘New Technology’ applying default options for ‘Sectorial Search’ and ‘Tree Fusing’ and setting 50 iterations of ‘Ratchet’ and 30 cycles of ‘Drift’. The Most Parsimonious Tree(s) (MPT) obtained was used as the starting point for a round of the Tree Bisection Reconnection (TBR) algorithm using the ‘Traditional search’ option. The Iter-PCR method (Pol and Escapa 2009) using the command ‘pcrprune’ (Goloboff and Szumik 2015) was employed to identify the rogue taxa. The resolution of the analyses was improved by excluding the rogue taxa (both a priori and a posteriori). Bremer Support values were calculated using the Bremer Support script and the Standard Bootstrap values (absolute frequencies) were calculated by applying the ‘Resampling’ function with 1000 replicates. Consistency (CI) and Retention (RI) indices were calculated utilizing the WSTATS script. Synapomorphies were obtained using the ‘Map Common synapomorphies’ option (File S1 [table S3]). We applied Equal Weighting (EW), and Implied Weighting (IW) setting the concavity constant ‘k’ to three and 12 (File S1 [table S2]). The analyses were conducted under two treatments (File S1 [table S2]): (1) considering all characters as unordered and (2) with multistate characters ordered (except char. 47 and 57).

Time-scaling was performed a posteriori using the function ‘bin\_timePaleoPhy’ of the package ‘paleotree’ (Bapst 2012) in the R library (R Core Team 2023). Default arguments were applied except for ‘type = equal’, ‘vartime = 0.1’, ‘ntrees = 1’, and ‘add.term = T’. The a posteriori time-scaling method used (type = equal) was developed by Brusatte et al. (2008). This method was originally outlined by Ruta et al. (2006) but modified later (Brusatte et al. 2008; Brusatte 2011). The time data of each taxon was treated as a column of precise first and last appearances (dateTreatment = firstLast). The tree topology is provided in Newick format (File S4). The interval times data used were obtained from the International Chronostratigraphic Chart v2023/09 (File S5). Finally, the first and last interval times of each OTU (FAD and LAD) (File S6) were based on the available bibliography (File S1 [1.3, and supplementary references therein]).

## Results

### Systematic palaeontology

**Dinosauria Owen, 1842 (sensu Langer et al. 2020)**

**Ornithischia Seeley, 1888 (sensu Madzia et al. 2021)**

**Thyreophora Nopcsa, 1915 (sensu Madzia et al. 2021)**

**Stegosauria Marsh, 1877 (sensu Madzia et al. 2021)**

**Stegosauridae Marsh, 1880 (sensu Madzia et al. 2021)**

**Neostegosauria nom. clad. nov.**

**Dacentrurinae Mateus, Maidment & Christiansen, 2009 (sensu this paper)**

***Dacentrurus* Lucas, 1902**

***Dacentrurus armatus* Owen, 1875**

**Synonymy.** *Omosaurus armatus* Owen, 1875, *Stegosaurus armatus* Lydekker, 1888, *Omosaurus lennieri* Nopcsa, 1911b, *Dacentrurus lennieri* Hennig, 1915b, *Dacentrurosaurus armatus* Hennig, 1925, *Miragaia longicollum* Mateus, Maidment & Christiansen, 2009, and *Dacentrurus longicollum* Raven & Maidment, 2017.

**Revised diagnosis.** *D. armatus* possesses the following autapomorphies (modified from Sánchez-Fenollosa et al. 2025): A premaxilla with (1) an anterior tip that drawn into a point; and (2) an anterolateral margin ventrally projected; a supraoccipital with (3) a posteroventrally orientation with an angle greater than 90° with the dorsal plane of the skull roof (new); a cervical series with (4) at least 17 cervical vertebrae; and (5) at least anterior and mid cervical ribs fused to the vertebrae; cervical vertebrae with (6) two spinopostzygapophyseal laminae that extend anterolaterally from the top of the postzygapophyses to both sides of the base of the neural spine and culminate on its anterior margin; mid and posterior cervical vertebrae with (7) neural spines positioned in the anterior half of the centrum; anterior caudal vertebrae with (8) short neural spines and expanded and rounded apices; an ilium with (9) a wide and short preacetabular process; and (10) a broad base of the preacetabular process and a smooth curvature between the anterior margin of the sacral yoke and the dorsal margin of the preacetabular process; and a pubis with (11) a dorsoventrally expanded anterior end of the prepubis.

**Holotype.** NHMUK PV OR46013 (Owen 1875; Galton 1985).

**Type locality and horizon.** Unknown horizon. The fossils were discovered in a clay pit at the municipality of Swindon (United Kingdom). Lower part of the Kimmeridge Clay Formation, Upper Jurassic (Kimmeridgian) (Davies 1876; Galton 1985; Martill et al. 2006).

**Referred material.** A partial cranium (MAP-9029) (Figs 2, 3) and a mid cervical vertebra (MAP-9030) (Fig. 4). Additional postcranial fossils of this specimen were recovered, but their study is beyond the scope of this research and some of them are still unprepared.

**Other referred material.** MHNHA (Nopcsa 1911b; Galton 1990), ML 433 (Fig. 6A–G; Mateus et al. 2009), ML 433-A (Mateus et al. 2009), MG 4863 (Costa and Mateus 2019), the Pedras Muitas specimen (Galton 1991; Escaso 2014), the Murteiras specimen (Galton 1991; Escaso 2014), the Atalaia specimen (Galton 1991; Escaso 2014), SHN.LPP 016 (Escaso et al. 2007b), the CO specimen (Casanovas-Cladellas et al. 1995), the RD-10 specimens (Cobos et al. 2010; Sánchez-Fenollosa et al. 2022), and the CT-28 specimen (Sánchez-Fenollosa et al. 2025).

**Locality and horizon.** Están de Colón (RD-34) site in the municipality of Riodeva, province of Teruel, Aragón, Spain. South-Iberian Basin, Villar del Arzobispo Formation, Upper Jurassic (upper Kimmeridgian–Tithonian) (Fig. 1).

**Locality and horizon of other referred material.** All specimens are known from the Upper Jurassic (Kimmeridgian–Tithonian) of western Europe (France, Portugal, and Spain) (Sánchez-Fenollosa et al. 2025 and references therein).

**Systematic remarks.** This stegosaurian specimen is classified as *D. armatus* because it possesses characters 5, 6, and 7 from the diagnosis. When coded as an independent OTU, it was recovered as sister to *D. armatus* in the phylogenetic analyses (File S1 [fig. S1]).

**Description.** **Cranium** (MAP-9029) (Figs 2, 3). MAP-9029 consist of the posterior half of the skull roof including a fragment of the right prefrontal, both frontals, both postorbitals, both squamosals, the parietal, the supraoccipital, and a possible fragment of the left paroccipital process (Figs 2, 3). The dorsal surface is slightly eroded and exhibits some cortical remodelling (Figs 2A, 3A). Perhaps for these reasons, sutures between elements are barely visible. Two small and open supratemporal fenestrae are present (Figs 2, 3A–D). Lateral temporal fenestrae presumably are large. Ventrally it is strongly eroded including almost all the braincase (Figs 2, 3). Each element of the cranium will be described individually below. — **Prefrontal.** A small fragment of the right prefrontal can be observed in posteromedially contact to the frontal (Figs 2, 3A–D). The suture with the frontal is barely visible (Figs 2, 3B). Its surface is flat and smooth (Figs 2A, 3A). Presumably, the non-preserved supraorbitals would exclude the prefrontal (also the frontal) from

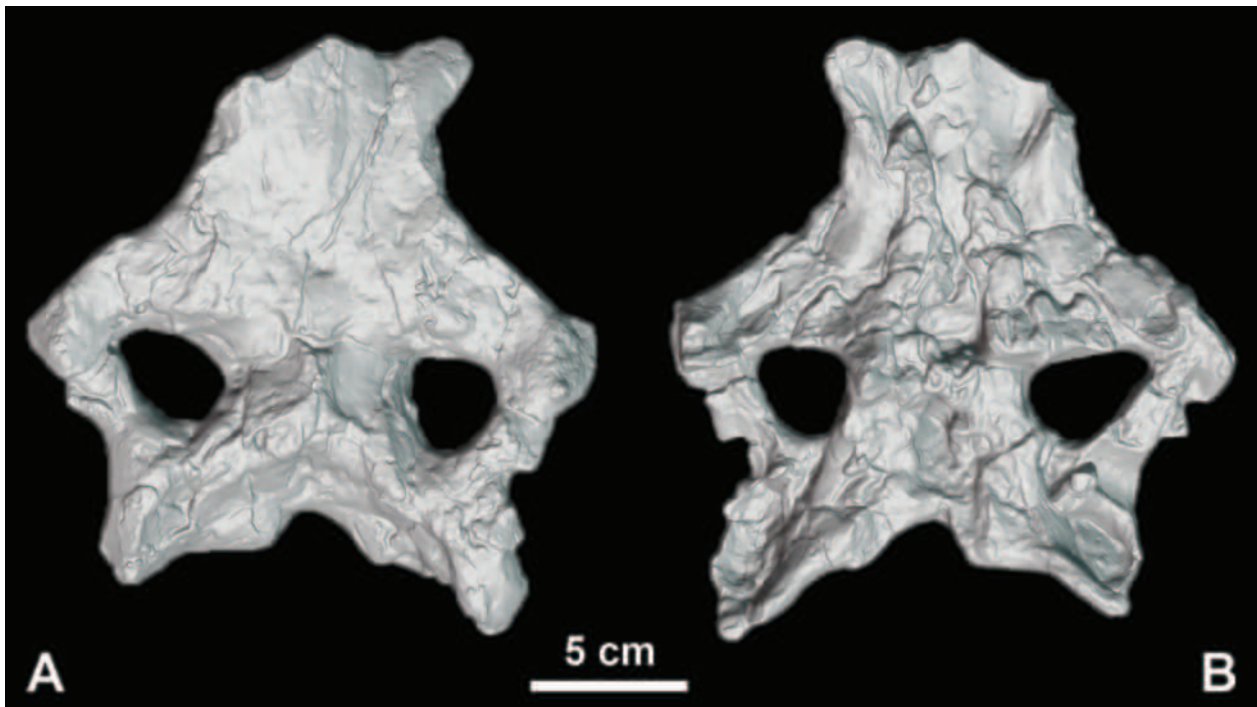


**Figure 2.** Cranium (MAP-9029) of *Dacentrurus armatus* Owen, 1875 from the Están de Colón (RD-34) fossil site (Riodeva, Teruel, Spain). 3D model of MAP-9029 in dorsal (A) and ventral (B) views. Produced and visualized using the Scantech iReal 2E scanner and IREAL 3D 2023 v. 3.3.3.3 software.

the orbital rim similar to that in other stegosaurs (e.g., Sereno and Dong 1992; Galton and Upchurch 2004; Salgado et al. 2017; Maidment et al. 2018; pers. obs. [NHMUK PV R36730]). — **Frontal.** Both frontals are present and they are longer than wide (Figs 2A, 3A, B) similar to that in *S. stenops* (Galton and Upchurch 2004; pers. obs. [NHMUK PV R36730]). Their surfaces are flat and the sagittal suture between them is straight and slightly convex (Figs 2A, 3A, B). The suture with postorbitals and parietal is barely visible in dorsal view (Figs 2A, 3A, B). — **Postorbital.** Both almost complete postorbitals are preserved and they form the anterolateral margins of the supratemporal fenestrae (Figs 2, 3A–D). The medial process is flat, broad and sutured to the frontal and parietal (excluding the frontal from the anteromedial margin of the supratemporal fenestra) (Figs 2, 3A–D) similar to that in *S. stenops* (Galton and Upchurch 2004; pers. obs. [NHMUK PV R36730]). The posterior process is slender and D-shaped in cross-section with a convex dorsal surface and a flattened ventral surface (Figs 2, 3A–D). The posterior process is in contact to the squamosal (Figs 2, 3A–D). The right postorbital preserves the most proximal part of the ventral process (Figs 2B, 3C) and dorsally in this area the postorbital is bulbous and exhibits a very small horn-like protuberance (Figs 2A, 3A). It is different from the bigger and more medially located protuberance of *H. taibaii* (Sereno and Dong 1992). — **Squamosal.** Both squamosals are present and triradiate (Figs 2, 3). They form the posterior margin of the supratemporal fenestrae and are in contact with the postorbital, parietal, and occiput (Figs 2, 3). The anterior process is short (Figs 2, 3A–D) and in the left squamosal it can be seen to underlap the postorbital (Figs 2B, C).

The posterior process is well-developed and horn-like (Figs 2, 3). In dorsal and ventral views, the lateral margin between posterior processes of postorbital and squamosal is concave (Figs 2, 3A–D). — **Parietal.** The parietal forms the medial margin of the supratemporal fenestrae (Figs 2, 3A–D). It is sub-square in dorsal view and its dorsal surface is convex with a straight and pronounced sagittal crest (Figs 2A, 3A, B) similar to that in *T. multispinus* (Dong et al. 1983). Distinct breaks in slope separate the dorsal surface from the lateral surfaces and the occiput (Figs 2, 3A–D). — **Occiput.** The upper-most part of the occiput is preserved and sutures between elements cannot be observed (Fig. 3E, F). The surface of the supraoccipital is smooth and there is not a dorsoventral ridge (Figs 2A, 3E, F) similar to that in *K. aethiopicus* (Galton 1988). The supraoccipital is obliquely oriented with an angle greater than  $90^\circ$  with the dorsal plane of the skull roof (Figs 2, 3A–D). A possible fragment of the left paroccipital process is preserved (Fig. 3E, F).

**Cervical vertebra** (MAP-9030) (Fig. 4). MAP-9030 is an almost complete mid cervical vertebra (Fig. 4). It is distorted and the anterior-most part is missing; therefore, some features and measurements must be considered cautiously. The centrum is presumably amphicoelous (Fig. 4C) and longer than wide and tall (File S1 [table S1]). The articular facets are wider than tall (File S1 [table S1]) and heart-shaped (Fig. 4A, C). Smooth concentric ridges are present in the surface of the posterior articular facet (Fig. 4C). Laterally, the parapophyses are located in the anterior margin and the upper half of the centrum (Fig. 4A, B, E). The ventral surface is smooth and concave due to the distortion (Fig. 4E). In general, the neural arch is

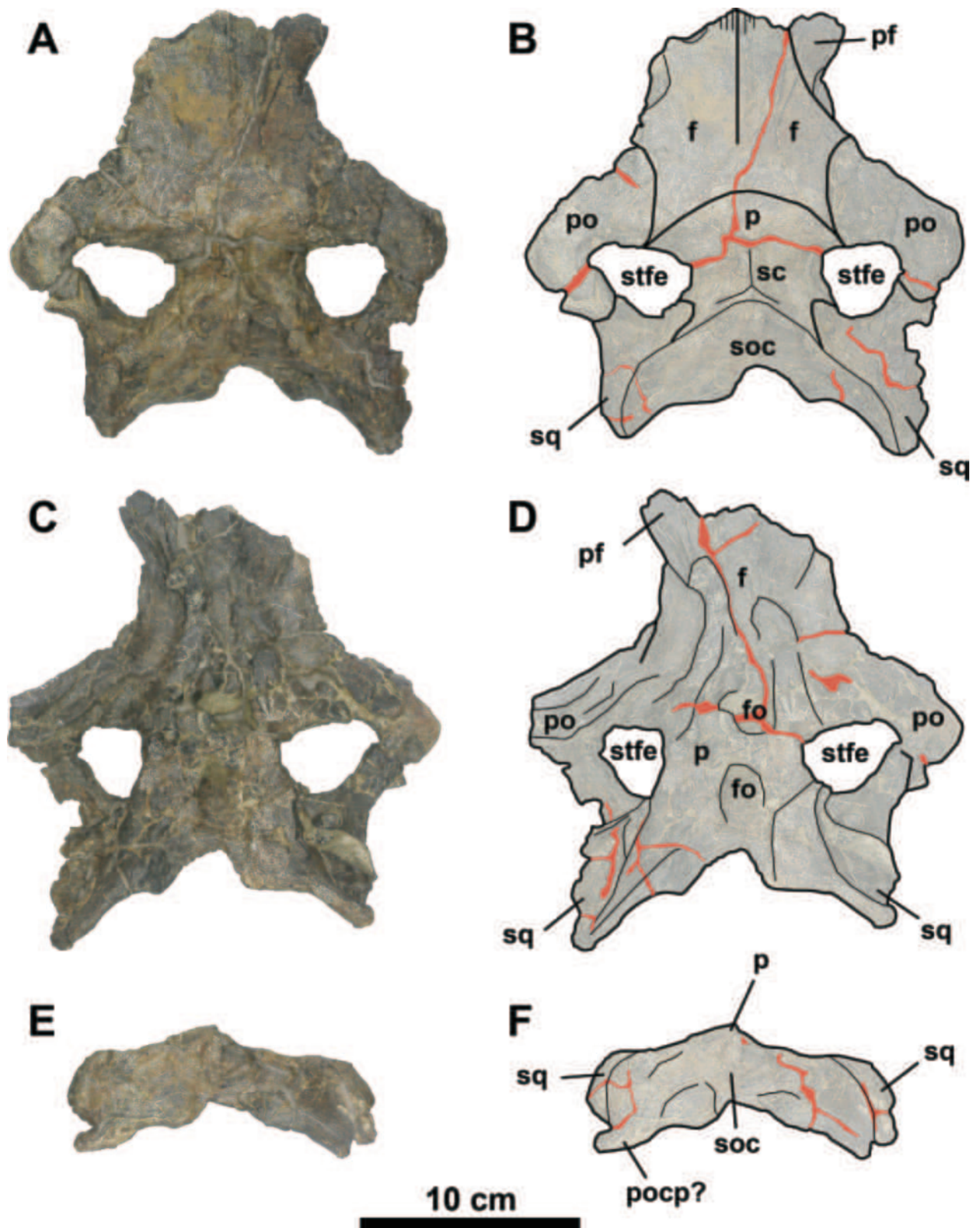


**Figure 3.** Cranium (MAP-9029) of *Dacentrurus armatus* Owen, 1875 from the Están de Colón (RD-34) fossil site (Riodeva, Teruel, Spain). Photographs (A, C, E) and interpretative drawings (B, D, F) of MAP-9029 in dorsal (A, B), ventral (C, D), and proximal (E, F) views. Abbreviations: f, frontal; fo, fossa; p, parietal; pocp, paroccipital process; po, postorbital; pf, prefrontal; sc, sagittal crest; soc, supraoccipital; sq, squamosal; stfe, supratemporal fenestra.

anteroposteriorly elongated and dorsally short (Fig. 4A–D). The neural canal is large and suboval (Fig. 4A, C). Regarding the prezygapophyses, only the posterior-most region is preserved and located below the postzygapoph-

yses (Fig. 4A, B, D). The diapophyses arise on the neural arch ventral to the prezygapophyses (Fig. 4A–C). Both cervical ribs are preserved and fused to the parapophyses and diapophyses of the vertebra (Fig. 4) similar to that

in *D. armatus* (Casanovas-Cladellas et al. 1995; Galton 1991; Mateus et al. 2009; Cobos et al. 2010; Costa and Mateus 2019; pers. obs. [ML 433 and CO specimen]), although only the left one is well-preserved (Fig. 4B). The left cervical rib is posteriorly directed, medially curved, notably overhang the centrum and has a blunt and round tip (Fig. 4B, D, E). The postzygapophyses are finger-like and extend beyond the posterior articular facet of the centrum (Fig. 4B–D). This differs from the greatly elongated postzygapophyses of *S. stenops* (Ostrom and McIntosh 1966; Escaso et al. 2007a; Maidment et al. 2015). Their articular facets are lateroventrally directed and oval in outline (Fig. 4B, C). Dorsally, two spinopostzygapophyseal laminae are well-visible, wide, and extending anterolaterally from the top of the postzygapophyses to both sides of the base of the neural spine and culminate on its anterior margin (Fig. 4D). This condition is shared with *D. armatus* (Mateus et al. 2009; Costa and Mateus 2019; pers. obs. [ML 433 and CO specimen]), but not with other stegosaurs (Ostrom and McIntosh 1966; Maidment et al. 2015; 2018; 2020; pers. obs. [NHMUK PV R37367 and NHMUK PV R37368]). The neural spine is located in the anterior half of the vertebra (Fig. 4B) and it is short and slightly transversely expanded (Fig. 4A, C) similar to that in *D. armatus* (Casanovas-Cladellas et al. 1995; Mate-

us et al. 2009; Costa and Mateus 2019; pers. obs. [ML 433 and CO specimen]). However, it is in the posterior half of the centrum (Gilmore 1914; Hennig 1925; Ostrom and McIntosh 1966; Dong et al. 1983; Zhou 1984; Galton 1990; Carpenter et al. 2001; Escaso et al. 2007a; Jia et al. 2007; Maidment et al. 2015; 2018) or in both halves (Maidment et al. 2020; pers. obs. [NHMUK PV R37367 and NHMUK PV R37368]) in other stegosaurian species.

## Phylogenetic nomenclature

### Neostegosauria Sánchez-Fenollosa & Cobos (nomen cladi novum)

**Registration number.** 1097.

**Phylogenetic definition.** The smallest clade containing *Kentrosaurus aethiopicus* Hennig, 1915a, *Dacentrurus armatus* Owen, 1875, and *Stegosaurus stenops* Marsh, 1887. This is a minimum-clade definition.

**Etymology.** Derived from ‘neo-’ (Greek), meaning new. And from the clade name Stegosauria.

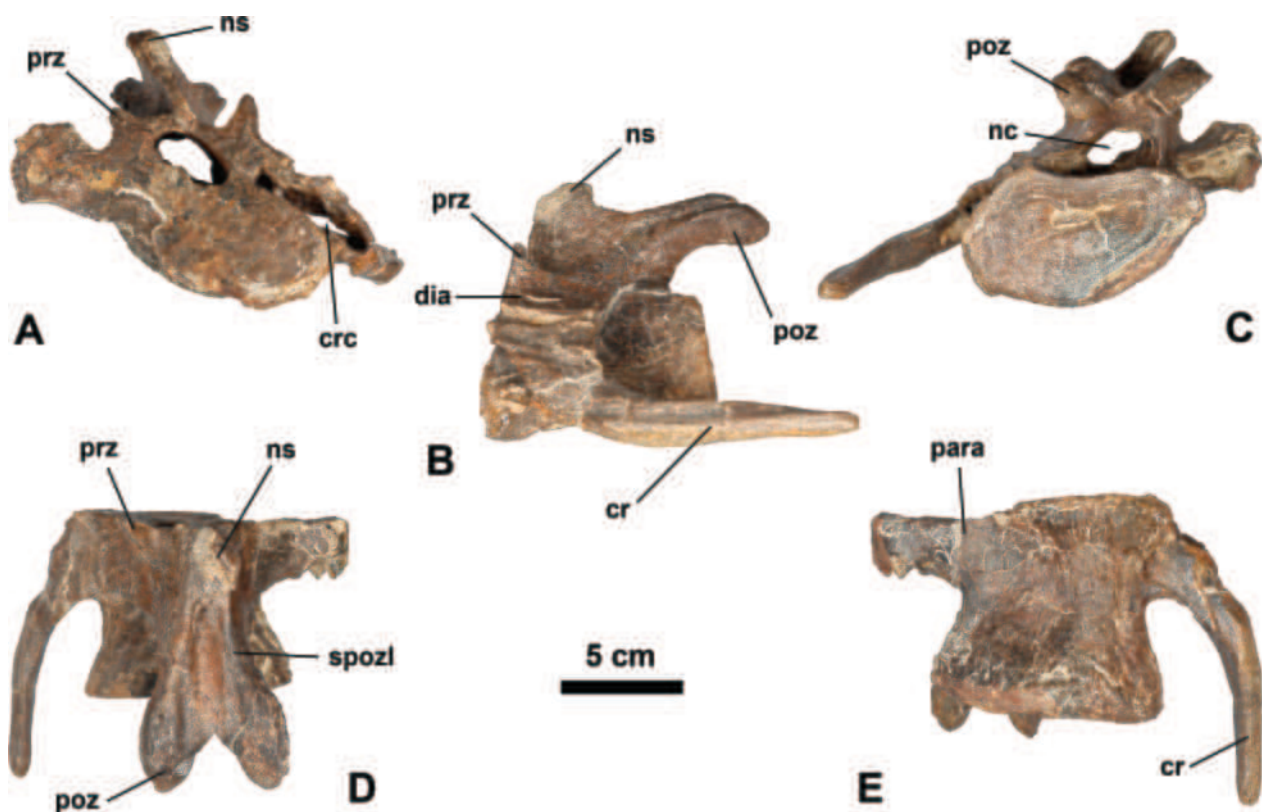


**Figure 4.** Mid cervical vertebra (MAP-9030) of *Dacentrurus armatus* Owen, 1875 from the Están de Colón (RD-34) fossil site (Riodeva, Teruel, Spain). Photographs (A–E) of MAP-9030 in anterior (A), left lateral (B), posterior (C), dorsal (D), and ventral (E) views. Abbreviations: cr, cervical rib; crc, cervical rib canal; dia, diapophysis; nc, neural canal; ns, neural spine; para, parapophysis; poz, postzygapophysis; prz, prezygapophysis; spozi, spinopostzygapophyseal lamina.

**Reference phylogeny.** Figure 5 of this paper is designated as the primary reference phylogeny. Additional reference phylogenies include figure 3.14 of Carpenter et al. (2001), figure 8 of Maidment et al. (2006), figure 1 of Raven and Maidment (2017), figure 12 of Maidment et al. (2020), figure 8 of Dai et al. (2022), figure 6 of Jia et al. (2024), figure 15 of Li et al. (2024a), figure 8 of Li et al. (2024b), figure 7 of Li et al. (2024c), and figure 12 of Zafaty et al. (2024).

**Composition.** According to the primary reference phylogeny, the clade Neostegosauria comprises *Lo. priscus*, *He. mjosi*, *S. stenops*, *J. junggarensis*, *W. homheni*, *Ya. ultimus*, *Al. longispinus*, *K. aethiopicus*, *Th. atlasicus*, *Ad. boulahfa*, and *D. armatus*.

**Comments.** Neostegosauria is the name established for the clade that includes the late-diverging members of Stegosauridae (Stegosaurinae and Dacentrurinae). This clade has been recovered in the last phylogenetic analyses although with differences in composition and topology. According to the primary reference phylogeny, it is supported by six synapomorphies (File S1 [1.6]). These synapomorphies, except the two cranial ones, are widely recognized in these taxa. Neostegosaurs are late-diverging stegosaurids of medium to large size that at least inhabited Africa and Europe during the Middle and Late Jurassic, North America during the Late Jurassic, and Asia during the Late Jurassic and Early Cretaceous. They are mainly characterized by presenting a dorsal process on the transverses processes of anterior and mid caudal vertebrae, and a solid sacral yoke with no foramina between ribs. Figure 5 of this paper has been designated as the primary reference phylogeny because it considers the latest taxonomic revisions, includes the highest number of stegosaurian OTUs, and provides a high-resolution topology.

### Stegosaurinae Marsh, 1880 (nomen cladi conversum)

**Registration number.** 1098.

**Phylogenetic definition.** The largest clade containing *Stegosaurus stenops* Marsh, 1887 but not *Dacentrurus armatus* Owen, 1875. This is a maximum-clade definition.

**Reference phylogeny.** Figure 5 of this paper is designated as the primary reference phylogeny. Additional reference phylogenies include figure 3.14 of Carpenter et al. (2001), figure 16.11 of Galton and Upchurch (2004), figure 8 of Maidment et al. (2006), figure 3 of Escaso et al. (2007a), figure 11A and 12A of Maidment et al. (2008), figure 1 of Mateus et al. (2009), figure 1 of Maidment (2010), figure 1 and 2 of Raven and Maidment (2017), figure 6A of Hao et al. (2018), figure 12 of Maidment et al. (2020), figure 8 of Dai et al. (2022), figure 6 of Jia et al. (2024), figure 15 of Li et al. (2024a), figure 8 of Li et al. (2024b), figure 7 of Li et al. (2024c), and figure 12 of Zafaty et al. (2024).

al. (2024b), figure 7 of Li et al. (2024c), and figure 12 of Zafaty et al. (2024).

**Composition.** According to the primary reference phylogeny, the clade Stegosaurinae comprises *Lo. priscus*, *He. mjosi*, *S. stenops*, *J. junggarensis*, *W. homheni*, and *Ya. ultimus*.

**Comments.** Stegosaurinae was first (informally) defined by Sereno (1998). Sereno (2005) defined Stegosaurinae applying the maximum-clade definition and using *S. stenops* as the internal specifier and *D. armatus* as the external specifier. This definition is formalized using the same type of definition and specifiers. Note that Raven et al. (2023) re-defined (informally) Stegosaurinae using *Stegosaurus* and *Hesperosaurus* Carpenter, Miles, and Cloward, 2001 as internal specifiers and a minimum-clade definition. There is no reason for its redefinition and makes it is less suitable. In fact, some authors have proposed the genus *Hesperosaurus* as a subjective junior synonym of *Stegosaurus*. Therefore, the ‘traditional concept’ of Stegosaurinae is retained. Figure 5 of this paper has been designated as the primary reference phylogeny because it considers the latest taxonomic revisions, includes the highest number of stegosaurian OTUs, and provides a high-resolution topology.

### Dacentrurinae Mateus, Maidment & Christiansen, 2009 (nomen cladi conversum)

**Registration number.** 1099.

**Phylogenetic definition.** The largest clade containing *Dacentrurus armatus* Owen, 1875 but not *Stegosaurus stenops* Marsh, 1887. This is a maximum-clade definition.

**Reference phylogeny.** Figure 5 of this paper is designated as the primary reference phylogeny. Additional reference phylogenies include figure 3.14 of Carpenter et al. (2001), figure 16.11 of Galton and Upchurch (2004), figure 8 of Maidment et al. (2006), figure 3 of Escaso et al. (2007a), figure 11A and 12A of Maidment et al. (2008), figure 1 of Mateus et al. (2009), figure 1 of Maidment (2010), figure 1 and 2 of Raven and Maidment (2017), figure 6A of Hao et al. (2018), figure 12 of Maidment et al. (2020), figure 8 of Dai et al. (2022), figure 6 of Jia et al. (2024), figure 15 of Li et al. (2024a), figure 8 of Li et al. (2024b), figure 7 of Li et al. (2024c), and figure 12 of Zafaty et al. (2024).

**Composition.** According to the primary reference phylogeny, the clade Dacentrurinae comprises *Al. longispinus*, *K. aethiopicus*, *Th. atlasicus*, *Ad. boulahfa*, and *D. armatus*.

**Comments.** Dacentrurinae was first (informally) defined by Mateus et al. (2009). This is formalized using the same

type of definition but replacing *S. armatus* Marsh, 1877 with *S. stenops* as external specifier. The species *S. armatus* was originally designated as the type species of the genus *Stegosaurus*, but it was later replaced by *S. stenops* as the type (International Commission on Zoological Nomenclature 2013). Figure 5 of this paper has been designated as the primary reference phylogeny because it considers the latest taxonomic revisions, includes the highest number of stegosaurian OTUs, and provides a high-resolution topology.

## Phylogenetic analysis

The new data matrix comprised 115 morphological characters and 30 OTUs (File S2), increasing to 31 OTUs when the specimen from RD-34 was coded as an independent OTU (File S3). The IterPCR method identified *M. exspectabilis* and *J. junggarensis* as rogue taxa. Multiple analyses (File S1 [table S2]) were conducted with the primary objective of identifying unstable regions of the tree (Fig. 5; File S1 [figs S3–S8]) and variations in the synapomorphies of the clades (File S1 [1.6]).

In the absence of rogue taxa exclusions, MP analyses recovered 10 MPTs (characters not ordered, multistate

characters ordered, and IW  $k = 12$ ) and 16 MPTs (IW  $k = 3$ ). The Strict Consensus Trees (SCTs) derived from these analyses exhibited poor resolution at the base of Stegosauria (File S1 [figs S3, S4]). However, when *M. exspectabilis* was excluded a posteriori, the resulting Reduced Strict Consensus Tree (RSCT) (File S1 [fig. S2]) was highly resolved and had a topology very similar to that of other analyses (Fig. 5; File S1 [1.5]).

MP analyses, excluding *M. exspectabilis* a priori, recovered a single MPT (Fig. 5) using unordered characters (194 steps, CI = 0.660, and RI = 0.799) and ordered multistate characters (196 steps, CI = 0.653, and RI = 0.803). When the analysis was conducted applying IW with  $k = 12$ , a single MPT was also recovered, but with a slightly different topology (File S1 [fig. S6]). However, when applying IW with  $k = 3$ , two MPTs were obtained, resulting in some changes to the topology and composition of Huayangosauridae and Stegosauridae (File S1 [fig. S5]). The same pattern is observed when the analyses were performed excluding both rogue taxa (File S1 [figs S7, S8]).

The topology (Fig. 5) obtained from the analyses 5 and 6 (File S1 [table S2]) was the most reliable for understanding stegosaurian evolutionary history due to its balance between high resolution (single MPT), min-

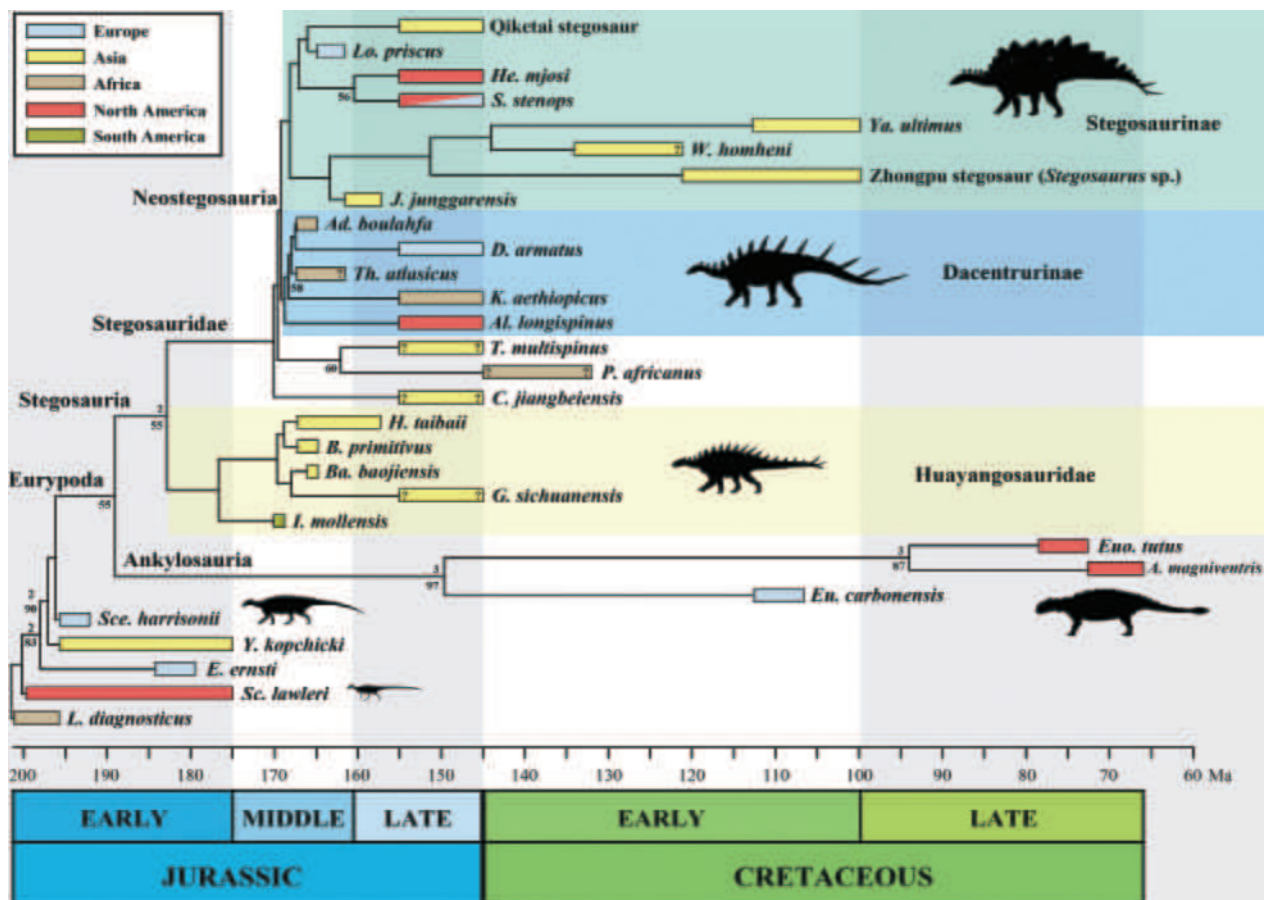


**Figure 5.** Chronogram showing temporal, palaeogeographical, and phylogenetic relationships of stegosaurian dinosaurs. Single MPT with a length of 194 steps. CI = 0.660 and RI = 0.799. The extremely fragmentary *Mongolostegus exspectabilis* Tumanova & Alifanov, 2018 was excluded a priori. Bremer Support values above (not showed values under 2) and Standard Bootstrap values below (not showed values under 50). The MPT was scaled in time a posteriori using the function ‘bin\_timePaleoPhy’ of the package ‘paleotree’ (Bapst 2012) in the R library (R Core Team 2023). Silhouettes obtained from PhyloPic.

imal exclusion of rogue taxa (only the extremely fragmentary *M. expectabilis*), and consistency with other alternative phylogenetic analyses (File S1 [1.5, 1.6]). Although some authors have suggested that IW parsimony outperforms EW (Goloboff et al. 2018; Ezcurra et al. 2023), others have pointed out that IW propagate errors and lead to reduced topological accuracy (Congreve and Lamsdell 2016; O'Reilly et al. 2016). In this context, EW parsimony remains the most widespread methodology applied in palaeontology, including in studies on stegosaurian dinosaurs.

*Sc. lawleri* was recovered as the most early-diverging thyreophoran included in these analyses (Fig. 5; File S1 [figs S2–S8]). *Sc. lawleri*, *E. ernsti*, *Y. kopchicki*, and *Sc. harrisonii* were excluded from Eurypoda (Ankylosauria + Stegosauria) (Fig. 5; File S1 [figs S2–S8]). The ankylosaurs *Eu. carbonensis*, *Euo. tutus*, and *A. magniventris* were recovered in a monophyletic group (Ankylosauria) and set as a sister group of Stegosauria (Fig. 5; File S1 [figs S2–S8]). When the extremely fragmentary *M. expectabilis* was excluded (both a priori and a posteriori), Stegosauria was highly resolved and formed by two major sister clades: Huayangosauridae and Stegosauridae (Fig. 5; File S1 [figs S2, S5–S8]). *M. expectabilis* was recovered as a huayangosaurid or an early-diverging stegosaurid (File S1 [figs S3, S4]).

According to the topologies obtained applying EW and IW with  $k = 12$ , Huayangosauridae included *I. mollensis*, *H. taibaii*, *B. primitivus*, *Ba. baojiensis*, and *G. sichuanensis* (Fig. 5; File S1 [figs S2, S6, S7]). *I. mollensis* was recovered as the most early-diverging huayangosaurid (Fig. 5; File S1 [figs S2, S6, S7]). *H. taibaii* and *B. primitivus*, and *Ba. baojiensis* and *G. sichuanensis* were recovered as sister taxa, respectively ([*H. taibaii* + *B. primitivus*] + [*Ba. baojiensis* + *G. sichuanensis*]) (Fig. 5; File S1 [figs S2, S6, S7]). Stegosauridae consisted of *C. jiangbeiensis* as the most early-diverging member (Fig. 5; File S1 [figs S2, S6, S7]), followed by a clade formed by *T. multispinus* and *P. africanus* (Fig. 5; File S1 [figs S2–S8]), and the newly defined clade Neostegosauria (Dacentrurinae + Stegosaurinae) (Fig. 5; File S1 [figs S2–S8]). However, in the IW analyses with  $k = 3$ , Huayangosauridae only included *I. mollensis*, *H. taibaii*, and *B. primitivus* in a polytomy (File S1 [figs S5, S8]), while *Ba. baojiensis* and *G. sichuanensis* were placed in Stegosauridae, forming a polytomy with *C. jiangbeiensis* and the clade formed by *T. multispinus* and *P. africanus* and Neostegosauria ([*T. multispinus* + *P. africanus*] + Neostegosauria) (File S1 [figs S5, S8]).

Stegosaurinae comprised two sister clades (Fig. 5; File S1 [figs S2–S8]). The first clade included the Qiketait stegosaur, *Lo. priscus*, *He. mjosi*, and *S. stenops* (Fig. 5; File S1 [figs S2–S8]). The second clade included *J. junggarensis*, the Zhongpu stegosaur, *W. homheni*, and *Ya. ultimus* (Fig. 5; File S1 [figs S2–S8]).

Finally, Dacentrurinae included *Al. longispinus*, *K. aethiopicus*, *Th. atlasicus*, *Ad. boulahfa*, and *D. armatus* (Fig. 5; File S1 [figs S2–S8]). In the analysis in which the specimen from RD-34 was treated as an independent OTU, it was grouped with *D. armatus* (File S1 [fig. S1]).

## Discussion

### Cranial anatomy of *Dacentrurus armatus* Owen, 1875 and character evolution

MAP-9029 (Figs 2, 3) exhibits a general morphology and a combination of characters typical of stegosaurian dinosaurs, including evidence of some cortical remodeling, the exclusion of the frontal from the dorsal orbital margin by the supraorbitals, and the presence of open supratemporal fenestrae. Stegosaurian cranial material from the Upper Jurassic of Europe is very scarce. Previous to this work, only two stegosaurian specimens preserve cranial elements (Fig. 6A–G; Mateus et al. 2009; Costa and Mateus 2019) and they have been referred to *D. armatus* (Sánchez-Fenollosa et al. 2025). ML 433 preserves a right premaxilla, a left maxilla, a left nasal, a postorbital fragment, and right and left angulars (Fig. 6A–G; Mateus et al. 2009). MG 4863 preserves an anterior fragment of the left dentary and an incomplete left quadrate (Costa and Mateus 2019). MAP-9029 (Figs 2, 3) consists of the most complete skull from the European stegosaurian fossil record. No overlapping cranial material exists between specimens, so they cannot be compared. However, this makes *D. armatus* one of the stegosaurs with a better-known skull anatomy.

*D. armatus* (Figs 2, 3A–D) and other stegosaurs such as the huayangosaurids *H. taibaii* (Fig. 7G), *I. mollensis* (Salgado et al. 2017), and *Ba. baojiensis* (Li et al. 2024b) and the stegosaurids *T. multispinus* (Maidment and Wei 2006), *He. mjosi* (Carpenter et al. 2001; Maidment et al. 2018), *S. stenops* (Fig. 7D, H), and *K. aethiopicus* (Galton 1988) exhibit the plesiomorphic character of open supratemporal fenestrae (char. 2.0) also present in early-diverging ornithischians such as *L. diagnosticus* (Fig. 7A) and early-diverging thyreophorans such as *Sc. lawleri* (Breedon and Rowe 2020), *E. ernsti* (Haubold 1990), *Y. kopchicki* (Yao et al. 2022), and *Sc. harrisonii* (Fig. 7B). This contrast with the apomorphic closed and/or covered supratemporal fenestrae (char. 2.1) observed in ankylosaurs (e.g., Fig. 7E; Arbour and Currie 2013; Leahey et al. 2015; Arbour and Mallon 2017; Xing et al. 2024).

Premaxillary teeth are present (char. 10.0) in huayangosaurids such as *H. taibaii* (Serenó and Dong 1992) and *I. mollensis* (Salgado et al. 2017). These retain the plesiomorphic condition of this character present in early-diverging ornithischians such as *L. diagnosticus* (Serenó 1991; Porro et al. 2015; pers. obs. [NHMUK PV R8501]), and early-diverging thyreophorans such as *Sc. lawleri* (Breedon et al. 2021), *E. ernsti* (Haubold 1990), and *Sc. harrisonii* (Norman 2020a). Edentulous premaxilla (char. 10.1) is present in stegosaurids such as *C. jiangbeiensis* (Dong et al. 1983), *P. africanus* (Raven and Maidment 2018; pers. obs. [NHMUK PV R47338]), *He. mjosi* (Siber and Mockli 2009), *S. stenops* (Fig. 6H, I), and *D. armatus* (Fig. 6A). Loss of premaxillary teeth allowed the development of a keratinous rhamphotheca (Czerkas



**Figure 6.** Cranial material of *Dacentrurus armatus* Owen, 1875 (ML 433, ‘*Miragaia longicollum*’ Mateus, Maidment & Christian-sen, 2009 holotype) from the Upper Jurassic of Portugal (A–G) and *Stegosaurus stenops* Marsh, 1887 (NHMUK PV R36730) from the Upper Jurassic of USA (H–K). Right premaxilla (A, B, H, I) in lateral (A, H), and ventral (B, I) views. Left maxilla (C, D, J) in lateral (C, J), and ventral (D) views. Left nasal (E, F, K) in lateral (E), and dorsal (F, K) views. Right angular (G) in lateral view. Abbreviations: en, external naris; ts, tooth socket. Numbers indicate the morphological character and its scoring.

1999). The acquisition of this feature has probably been homoplastic between stegosaurs and ankylosaurs because early-diverging taxa of both groups have toothed premaxilla (e.g., Carpenter et al. 1998). Neostegosaurs such as *D. armatus* (Fig. 6B) and *S. stenops* (Figs 6I, 7G) have a broad notch between premaxillae on the midline (char. 5.1). However, it is absent (char. 5.0) in the early-diverging ornithischian *L. diagnosticus* (Sereno 1991;

pers. obs. [NHMUK PV R8501]), in the early-diverging thyreophorans *Sc. lawleri* (Breedon et al. 2021) and *Sc. harrisonii* (Norman 2020a), and in the huayangosaurid *H. taibaii* (Fig. 7G; Sereno and Dong 1992). Therefore, huayangosaurids retain the plesiomorphic condition. The premaxilla of *D. armatus* (Fig. 6A) has an elongated nasal process that forms the anterodorsal margin of the external naris (char. 7.1) similar to the stegosaurids *C. jiangbei-*

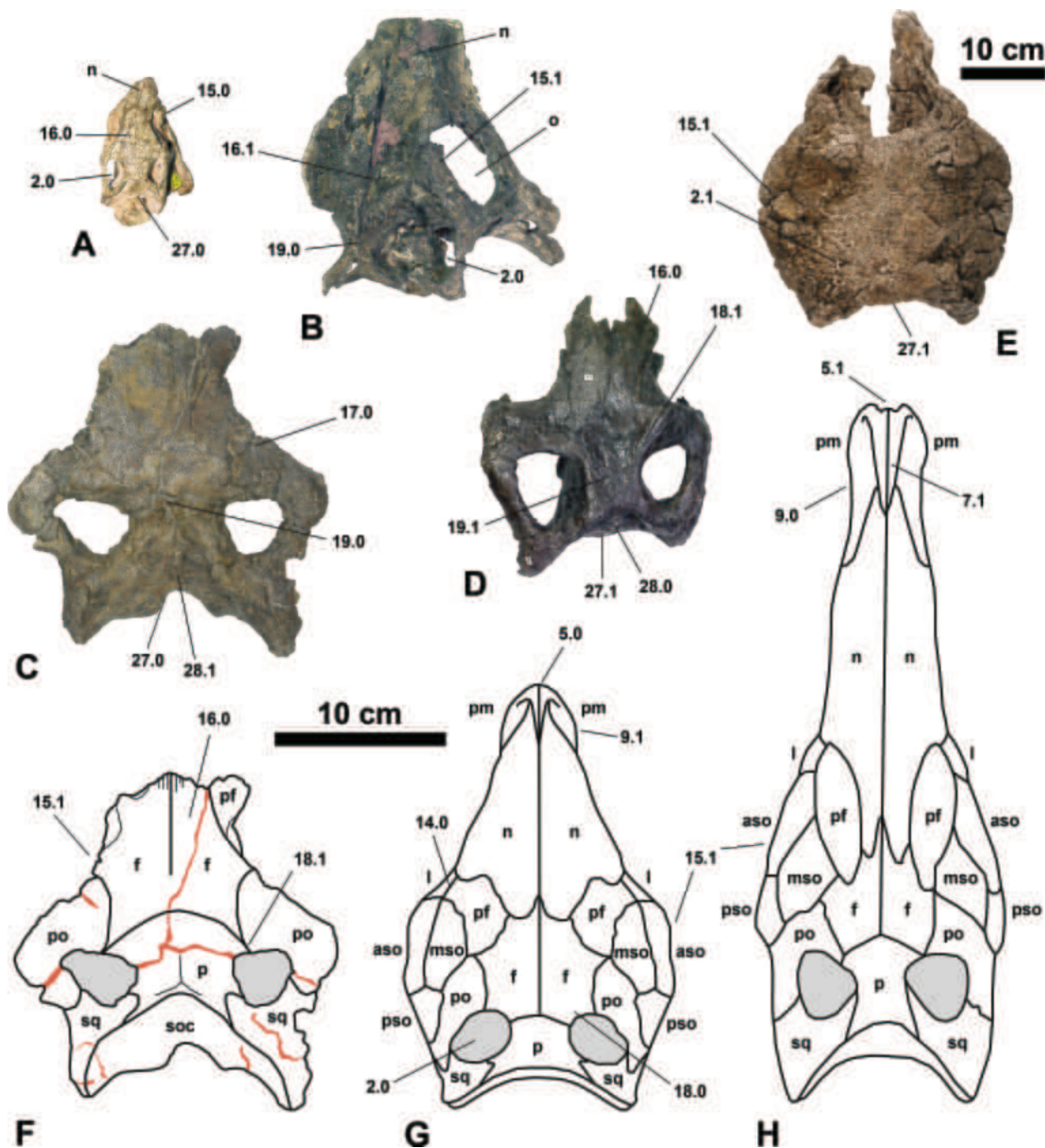


**Figure 7.** Skulls of ornithischian dinosaurs (A–E) and interpretative drawings in dorsal view (F–H). **A.** *Lesothosaurus diagnosticus* Galton, 1978 (NHMUK PV RU B23). **B.** *Scelidosaurus harrisonii* Owen, 1861 (NHMUK PV R1111). **C, F** *Dacentrurus armatus* Owen, 1875 (MAP-9029). **D.** *Stegosaurus stenops* Marsh, 1887 (NHMUK PV R36730). **E.** *Europelta carbonensis* Kirkland et al., 2013 (AR-1-544/10). **G.** *Huayangosaurus taibaii* Dong, Tang & Zhou, 1982 (modified from Sereno and Dong 1992). **H.** *S. stenops* (modified from Galton and Upchurch 2004). Abbreviations: aso, anterior supraorbital; f, frontal; l, lacrimal; mso, medial supraorbital; n, nasal; o, orbit; p, parietal; pf, prefrontal; pm, premaxilla; po, postorbital; pso, posterior supraorbital; sq, squamosal; stfe, supratemporal fenestra. Numbers indicate the morphological character and its scoring.

*ensis* (Dong et al. 1983; Galton and Upchurch 2004) and *S. stenops* (Figs 6H, 7G). This contrast to the condition observed in the early-diverging ornithischian *L. diagnosticus* (Serenio 1991), the early-diverging thyreophoran *Sc. lawleri* (Breedon et al. 2021), and the huayangosaurid *H. taibaii* (Serenio and Dong 1992), which nasal process only forms the anterior margin of the external naris (char. 7.0). Moreover, the huayangosaurid *H. taibaii* has an abbreviated subnarial portion (char. 9.1) (Fig. 7G), whereas neostegosaurs such as *D. armatus* (Fig. 6A) and *S. stenops* (Figs 6H, 7G) have an elongated subnarial portion (char. 9.0). Therefore, probably huayangosaurids displayed massive and short premaxilla and stegosaurids acquired a slender and elongated premaxilla in their evolutionary history.

Most of stegosaurs, including *D. armatus* (Fig. 6C, D), exhibit a maxillary tooth row inset medially (char. 13.1). This condition derived from the tooth row in line with the lateral edge of the premaxilla (char. 13.0) present in early-diverging ornithischians such as *L. diagnosticus* (Serenio 1991; Porro et al. 2015; pers. obs. [NHMUK PV RU B17, NHMUK PV RU B23, NHMUK PV R8501, and NHMUK PV R11956]), and in early-diverging thyreophorans such as *Sc. lawleri* (Breedon et al. 2021) and *E. ernsti* (Haubold 1990). The early-diverging thyreophorans *Y. kopchicki* (Yao et al. 2022) and *Sc. harrisonii* (Norman 2020a; pers. obs. [NHMUK R1111]) also has tooth row inset medially like most of stegosaurs revealing that this feature was acquired at an early stage of the evolution of thyreophorans. In general, ankylosaurs exhibit deep buccal emarginations (char. 13.2). Therefore, the condition observed in *T. multispinus* (Maidment and Wei 2006) and *P. africanus* (Raven and Maidment 2018; pers. obs. [NHMUK PV R47338]) probably consist of a derived trait and is homoplastic (char. 13.0).

In *D. armatus* (Figs 2, 3A–D), as well as in other stegosaurs such as *H. taibaii* and *S. stenops* (Fig. 7D, G, H), the frontal is excluded from the orbital rim (char. 15.1). This also occurs in early-diverging thyreophorans such as *Y. kopchicki* (Yao et al. 2022) and *Sc. harrisonii* (Fig. 7B) and ankylosaurs (e.g., Fig. 7E; Arbour and Currie 2013; Leahey et al. 2015; Arbour and Mallon 2017; Xing et al. 2024). However, early-diverging ornithischians such as *L. diagnosticus* (Fig. 7A) and the early-diverging thyreophorans *Sc. lawleri* (Breedon and Rowe 2020) and *E. ernsti* (Haubold 1990) exhibit a frontal that form the dorsal margin of the orbit. Moreover, they have a free and rod-like palpebral bone (char. 15.0). The incorporation of the palpebral bone into the skull roof as supraorbital elements is responsible for the exclusion of the frontal from the dorsal margin of the orbit in *Y. kopchicki*, *Sc. harrisonii*, ankylosaurs, and stegosaurs (Maidment and Porro 2010). The frontal of *D. armatus* (Figs 2A, 3A, B) is longer than wide (char. 16.0) and is excluded from the anterior margin of the supratemporal fenestra (char. 18.1) similar to that in *S. stenops* (Fig. 7D, H). These probably represent apomorphic characters derived from the equidimensional or wider than long frontal (char. 16.1) and a postorbital that does not contact the parietal (char. 18.0) present in huayangosaurids (Fig. 7G; Sereno and

Dong 1992; Salgado et al. 2017; Li et al. 2024b) and in non-neostegosaurian stegosaurids such as *T. multispinus* (Maidment and Wei 2006).

The parietal of *D. armatus* (Figs 2A, 3A, B) is convex (char. 19.0) with a remarkably sagittal crest. This condition is more similar to that in *T. multispinus* (Dong et al. 1983) than to the flat dorsal surface (char. 19.1) of the huayangosaurid *H. taibaii* (Serenio and Dong 1992), and the neostegosaurs *K. aethiopicus* (Galton 1988), *He. mjosi* (Carpenter et al. 2001; Maidment et al. 2018), and *S. stenops* (Fig. 7D). In extant mammals, the sagittal crest has been evolved independently in several lineages. Generally, it allows attachment for larger temporalis muscles, providing higher bite force and/or increased masticatory processing of tough food (e.g., Tanner et al. 2008; Figueirido et al. 2014; DeSantis et al. 2020). Therefore, the presence of a sagittal crest might have enabled *D. armatus* to chew for longer periods, which would be particularly beneficial when consuming tough foods with low nutritional value. However, in this case, the sagittal crest is relatively small, and a detailed functional study will be necessary to confirm this hypothesis.

The supraoccipital of *D. armatus* (Figs 2, 3) is posteroventrally oriented and clearly visible in dorsal view (char. 27.0). This condition contrast with the ventrally oriented supraoccipital that forms an angle of 90° with the dorsal plane of the skull roof (char. 27.1) present in other stegosaurs (Fig. 7D; Dong et al. 1983; Galton 1988; Sereno and Dong 1992; Galton and Upchurch 2004; Maidment et al. 2018). Therefore, it is likely to be an autapomorphic character for *D. armatus*. The extremely elongated neck and the axial muscles attachment may be related functionally with this cranial feature. Furthermore, this feature probably has implications for the position and orientation of the skull.

Finally, the dorsoventral ridge present in the supraoccipital (char. 28.0) of early-diverging ornithischians such as *L. diagnosticus* (Serenio 1991; Porro et al. 2015; pers. obs. [NHMUK PV RU B23]), early-diverging thyreophorans such as *Y. kopchicki* (Yao et al. 2022) and *Sc. harrisonii* (Norman 2020a; pers. obs. [NHMUK PV R1111]), and some stegosaurs (Fig. 7D; Sereno and Dong 1992; Dong et al. 1983; Galton and Upchurch 2004; Maidment et al. 2018), disappears (char. 28.1) in the dacentrurines *K. aethiopicus* (Galton 1988) and *D. armatus* (Figs 2A, 3E, F).

## Stegosaurian evolutionary history: taxonomic and phylogenetic implications

Madzia et al. (2021) formalized three pre-existing stegosaurian clade names (Stegosauria, Huayangosauridae, and Stegosauridae). However, they did not formalize other pre-existing clade names like Stegosaurinae (Serenio 2005) and Dacentrurinae (Mateus et al. 2009). These clades have been recovered in many phylogenetic analyses but with different compositions and topologies (e.g., Carpenter et al. 2001; Galton and Upchurch

2004; Maidment et al. 2008; Raven and Maidment 2017; Jia et al. 2024), making it challenging to compare results among studies. Establishing formal definitions for these groups helps standardize terminology and improves clarity when discussing phylogenetic relationships. For this reason, Stegosaurinae and Dacentrurinae are formalized by following the requirements and recommendations of the PhyloCode and keeping the original and traditional concept. Moreover, a new clade name, Neostegosauria, is proposed. Neostegosauria includes the late-diverging members of Stegosauridae and it has been also recovered in other analyses but with varying composition and topology (e.g., Carpenter et al. 2001; Raven and Maidment 2017; Dai et al. 2022; Jia et al. 2024; Li et al. 2024a, 2024c). According to the MP analyses, neostegosaurs are characterized by the possession of the following synapomorphies (File S1 [table S3]): (1) a frontal that is longer than wide (char. 16.0), (2) a medial process of the postorbital that contacts with the parietal (char. 18.1), (3) anterior and mid caudal vertebrae with a dorsal process on the transverse processes (char. 62.1), a scapula with (4) a subquadrangular acromial process with a posterodorsal corner (char. 72.1) and (5) a parallel sided blade (char. 73.1), and a sacral yoke with (6) large foramina between ribs (char. 86.1). An additional synapomorphy (char. 33.0) is recognized when the rogue taxon *J. junggarensis* was excluded from the analyses (File S1 [table S3]). Defining these phylogenetic names not only ensures consistency but also facilitates communication, discussion, and comparison between stegosaurian evolutionary hypotheses.

Raven and Maidment (2017) incorporated continuous characters into their data matrix to improve tree resolution. However, they did not account for intraspecific variation or variation within the same series in the case of the axial skeleton. Continuous characters significantly influence inferred evolutionary relationships, over 50% of apomorphic characters correspond to continuous characters (e.g., Raven and Maidment 2017; Jia et al. 2024; Li et al. 2024b), despite these representing only 20% of the total characters. Therefore, misapplication of continuous characters, along with other occasional errors, likely explains why MP analyses based on this data matrix and its derivatives (Maidment et al. 2020; Dai et al. 2022; Jia et al. 2024; Li et al. 2024b, 2024c; Zafaty et al. 2024), produce notably longer and more homoplastic trees than those presented here. This also explains certain inconsistencies with fossil evidence, direct comparisons, and taxonomy. For instance, recent phylogenetic analyses (e.g., Raven and Maidment 2017; Maidment et al. 2020; Dai et al. 2022; Li et al. 2024b) did not recover the holotypes of *D. armatus* and ‘*Mi. longicollum*’ as sister taxa because the continuous characters related to the proportions of dorsal vertebrae for ‘*Mi. longicollum*’ were coded solely based on the preserved first and second dorsal vertebrae (see Sánchez-Fenollosa et al. 2025 for details).

CI and RI values from MP analyses are higher than those reported in recent analyses (e.g., Raven and Maidment 2017; Dai et al. 2022; Jia et al. 2024; Li et al. 2024a,

2024b). This implies that these analyses potentially have greater coherence between morphological characters and inferred phylogenetic relationships. However, Bremer Support and Bootstrap values are similar to those in other analyses (e.g., Raven and Maidment 2017; Jia et al. 2024; Li et al. 2024a, 2024b). These low values indicate weak robustness and confidence for most stegosaurian clades. This trend across stegosaurian phylogenetic analyses may result from the fact that most species are represented by a single partial skeleton and highly incomplete material. Therefore, fieldwork and new fossil discoveries will be crucial for advancing the understanding of stegosaurian evolutionary history.

Several synapomorphies support the major clades of Thyreophora, Ankylosauria, and Stegosauria (File S1 [table S3]). However, this new data matrix only includes a few non-stegosaurian taxa (Table 1; File S2). Therefore, these synapomorphies (File S1 [table S3]) are limited and should be considered with caution. The taxa *Sc. lawleri* (Kayenta Formation, Sinemurian–Toarcian, USA), *E. ernsti* (Posidonienschiefer Formation, early Toarcian, Germany), *Y. kopchicki* (Fengjiahe Formation, late Sinemurian–Toarcian, China), and *Sc. harrisonii* (Charmouth Mudstone Formation, late Sinemurian, UK) are clearly outside of Eurypoda and are considered early-diverging thyreophorans (Fig. 5; File S1 [figs S2–S8]). Other authors obtained similar results studying the evolutionary relationships of ornithischians and thyreophorans (e.g., Sereno 1999; Thompson et al. 2012; Baron et al. 2017; Raven and Maidment 2017; Han et al. 2018; Dieudonné et al. 2021; Raven et al. 2023; Fonseca et al. 2024). However, these results differ from those of Wiersma and Irmis (2018), in which *Sc. harrisonii* is recovered as an ankylosaur, and Norman (2021), in which *Sc. lawleri*, *E. ernsti* and *Sc. harrisonii* are recovered as ankylosauromorphans (= ankylosaurs sensu Madzia et al. 2021).

The time-scaled tree suggests that first stegosaurs may have appeared during the Early Jurassic and declined, coincident with the rise of ankylosaurs, in the Early Cretaceous (Fig. 5). Cretaceous stegosaurs are represented by a handful of valid taxa: *M. exspectabilis*, *W. homheni*, *Ya. ultimus* from Asia (Dong 1990; Tumanova and Alifanov 2018; Jia et al. 2024) and *P. africanus* from Africa (Raven and Maidment 2018). Fragmentary stegosaurian remains have been reported from at least the Lower Cretaceous of Europe (Galton 1981; Pereda-Suberbiola et al. 2003; Al-lain et al. 2022) and South America (Pereda-Suberbiola et al. 2013), and the Upper Cretaceous of India (Yadagiri and Ayyasami 1979).

*I. mollensis* was originally interpreted as an early-diverging ornithopod (Salgado et al. 2017). However, it is here recovered as a stegosaur (Fig. 5; File S1 [figs S2–S8]) and is included within the clade Huayangosauridae (Fig. 5; File S1 [figs S2, S5–S8]). This taxon exhibits several features shared with other huayangosaurids and early-diverging stegosaurids: (1) large antorbital fossa (char. 3.0; shared with *H. taibaii*), (2) presence of premaxillary teeth (char. 10.0; shared with *H. taibaii*), (3) presence of an anterior maxillary foramen (char. 12.1;

shared with *H. taibaii*), (4) asymmetrical tooth crown (char. 36.0; shared with *H. taibaii*, *G. sichuanensis*, and *C. jiangbeiensis*), (5) > 25 maxillary/dentary teeth (char. 38.2; shared with *H. taibaii* and *G. sichuanensis*), and (6) weakly developed cingulum (char. 39.0; shared with *H. taibaii*). Other authors have also suggested that *I. mollensis* is a stegosaur (Han et al. 2018; Raven and Maidment 2018; Raven et al. 2023; Fonseca et al. 2024). The type specimen of *I. mollensis* is not fully prepared, so further work on this specimen and the discovery of new fossils may allow a better understand of the evolutionary relationships of this species. *I. mollensis* is especially important because it is the oldest known stegosaurian taxon and the first described from South America (lower Bajocian, Argentina). Fragmentary stegosaurian specimens have been also found in the Upper Jurassic and Lower Cretaceous of South America (Pereda-Suberbiola et al. 2013; Rauhut et al. 2021).

*M. exspectabilis* has been included for the first time in a stegosaurian phylogenetic analysis and it is recovered as a huayangosaurid or an early-diverging stegosaurid (File S1 [figs S3, S4]). This taxon was described from very fragmentary material: six caudal vertebrae, two partial pubes, and a fragment of a sacral rib (Tumanova and Alifanov 2018). However, *M. exspectabilis* exhibits some features exclusively present in huayangosaurids and early-diverging stegosaurids: anterior and mid caudal vertebrae with (1) transverse processes without dorsal process (char. 62.0) and (2) neural spines with unexpanded apex (char. 66.0), and a pubis with (3) a dorsal edge of the postpubis without a kink (char. 94.0). It was found in beds of the Dzundain Formation (Mongolia, Asia) with an age of Lower Cretaceous (Aptian–Albian). Therefore, *M. exspectabilis* is one of the youngest stegosaurs currently known and these results suggest that a lineage of huayangosaurids or early-diverging stegosaurids persisted in Asia until at least the late Early Cretaceous.

The MP analyses recovered Huayangosauridae and Stegosauridae with small variations in composition and topology depending on the methodology applied (Fig. 5; File S1 [figs S2, S5–S8]). In most analyses (Fig. 5; File S1 [table S2; figs S2, S6, S7]), Huayangosauridae includes *I. mollensis* (Los Molles Formation, early Bajocian, Argentina), *H. taibaii* (lower Shaximiao Formation, Bathonian–early Oxfordian, China), *B. primitivus* (lower Shaximiao Formation, Bathonian, China), *Ba. baojiensis* (Wangjiashan Formation, late Bathonian, China), and *G. sichuanensis* (upper Shaximiao Formation, ?Kimmeridgian–?Tithonian, China) and it is supported by two synapomorphies (File S1 [table S3]): (1) presence of an anterior maxillary foramen (char. 12.1) and (2) > 25 maxillary/dentary teeth (char. 38.2). These results clearly differ from those of recent phylogenies (e.g., Hao et al. 2018; Maidment et al. 2020; Dai et al. 2022; Jia et al. 2024; Li et al. 2024b; Zafaty et al. 2024). However, they resemble those obtained by Li et al. (2024a) although *C. jiangbeiensis* and *T. multispinus* are recovered here as early-diverging members of Stegosauridae (Fig. 5; File S1 [figs S2, S5–S8]). The clade Stegosauridae is supported by two synapomorphies (File S1 [table S3]): a premaxilla with

(1) an elongated nasal process that forms the anterodorsal margin of the external naris (char. 7.1) and a femur with (2) a fourth trochanter extremely reduced or inappreciable (char. 99.2). An additional synapomorphy (char. 51.2) is recognized when the multistate characters were treated as ordered (File S1 [table S3]). *C. jiangbeiensis* (upper Shaximiao Formation, ?Kimmeridgian–?Tithonian, China) is the earliest-diverging member and it retains some simpliomorphic characters such as (1) asymmetrical tooth crowns (char. 36.0) and (2) neural spines of anterior and mid caudal vertebrae with unexpanded apex (char. 66.0).

When applying IW with  $k = 3$ , Huayangosauridae is more restricted, including only *I. mollensis*, *B. primitivus*, and *H. taibaii* (File S1 [figs S5, S8]), and is supported solely by the presence of an anterior maxillary foramen (char. 12.1) (File S1 [table S3]). In contrast, *Ba. baojiensis* and *G. sichuanensis* are recovered as early-diverging members of Stegosauridae (File S1 [figs S5, S8]), a clade supported in this case by the presence of (1) maxillary and dentary teeth with a greatly developed and ring-like cingulum (char. 39.1) and (2) cervical vertebrae with postzygapophyses elongated that slightly overhang the centrum facet (char. 45.1) (File S1 [table S3]).

*T. multispinus* (upper Shaximiao Formation, ?Kimmeridgian–?Tithonian, China) and *P. africanus* (Kirkwood Formation, ?Berriasian–?Valanginian, South Africa) exhibit a single synapomorphy: maxillary tooth row in line with the lateral edge of the premaxilla (char. 13.0). Both species have been recovered as sister taxa in some recent phylogenetic analyses (e.g., Raven and Maidment 2017; Dai et al. 2022; Jia et al. 2024; Zafaty et al. 2024). However, as noted Raven et al. (2023), this is likely due to a combination of missing data (*P. africanus* is extremely fragmentary) and similarities in tooth morphology (also present in other stegosaurs).

Neostegosauria is supported by several synapomorphies (see above and File S1 [table S3]) and is formed by Stegosaurinae and Dacentrurinae (Fig. 5; File S1 [figs S2–S8]). The first neostegosaurs (Fig. 5) appeared in the Middle Jurassic, suggesting that stegosaurs diversified rapidly during this epoch.

Stegosaurinae, comprising exclusively Laurasian taxa, exhibits a stable composition across all analyses (Fig. 5; File S1 [figs S2–S8]), although its synapomorphies vary depending on the methodology applied (File S1 [table S3]). This clade is invariably supported by two synapomorphies (File S1 [table S3]): dermal armour with (1) a parasagittal arrangement of rows alternating on each side of the midline (char. 110.1) and (2) dorsal plates with a generally thin structure (char. 112.1). A third synapomorphy (char. 37.0) is present in most analyses but is either absent or substituted (char. 64.1) under IW with  $k = 3$  (File S1 [table S3]). When the rogue taxa *J. junggarensis* was excluded a priori, Stegosaurinae is supported by a single synapomorphy (char. 112.1) (File S1 [table S3]). Some stegosaurs exhibit variations in plate morphology that have been interpreted as potential evidence of sexual dimorphism (Saitta 2015). However, the synapomorphies supporting this clade, as well as the dermal plate

characters incorporated in this data matrix, do not pertain to plate morphology. If these interpretations are correct, such variations likely reflect interspecific differences rather than phylogenetic signals.

In turn, Stegosaurinae is divided into two main lineages (Fig. 5; File S1 [figs S2–S8]). The first of them includes *J. junggarensis* (Shishugou Formation, early Oxfordian, China), *W. homheni* (late Valanginian–?Barremian, Lianmuqin and Jingchuan Formations, China), *Ya. ultimus* (Albian, Zuoyun Formation, China), and the Zhongpu stegosaur (Aptian–Albian, upper Hekou Group, China). In most analyses, this clade is supported by a single synapomorphy: some cervical centra with a remarkably foramen on lateral surface (char. 43.1). This character is present in *J. junggarensis* (Jia et al. 2007) and in the Zhongpu stegosaur (Li et al. 2024c), but unknown in *W. homheni* (Dong 1990) and *Ya. ultimus* (Jia et al. 2024). Additionally, *W. homheni*, *Ya. ultimus*, and the Zhongpu stegosaur share the presence of dorsal neural arches with anterior and posterior surfaces deeply excavated above the neural canal (char. 52.1, [?] in *J. junggarensis*). This character supports this clade under analyses 4 and 7 (File S1 [table S2]). Maidment et al. (2008) synonymized the genera *Wuerhosaurus* Dong, 1973 and *Stegosaurus* and diagnosed *S. homheni* based on a single autapomorphy (char. 52.1 here). However, the results of this study (Fig. 5; File S1 [figs S2–S8]) clearly distinguish the species *W. homheni* and *S. stenops*, leading us to recognize *Wuerhosaurus* and *Stegosaurus* as separate genera. Therefore, the Zhongpu stegosaur, originally referred to *Stegosaurus* sp. (Li et al. 2024c), requires taxonomic re-evaluation. Moreover, the presence of dorsal neural arches with anterior and posterior surfaces deeply excavated above the neural canal (char. 52.1; autapomorphy of *W. homheni* sensu Maidment et al. 2008) in both *Ya. ultimus* and the Zhongpu stegosaur supports the need for a taxonomic revision of Early Cretaceous Chinese stegosaurs.

The second lineage of stegosaurines (Fig. 5; File S1 [figs S2–S8]) includes the Qiketai stegosaur (Kimmeridgian–Tithonian, Qigu Formation, China), *Lo. priscus* (Callovian, Oxford Clay Formation and unnamed unit, UK and France), *He. mjosi* (Kimmeridgian–Tithonian, Morrison Formation, USA), and *S. stenops* (Kimmeridgian–Tithonian, Morrison and Lourinhã Formations, USA and Portugal) and it is supported by two synapomorphies: anterior and mid caudal vertebrae (posterior to Cd2) with (1) transverses processes greatly ventrally projected (char. 61.1) and a coracoid with (2) subcircular morphology (char. 68.1). In most analyses, the Qiketai stegosaur and *Lo. priscus* are recovered as sister OTUs (Fig. 5; File S1 [figs S2, S3, S6, S7]) consistent with Li et al. (2024a). The Morrison Formation stegosaurs, *He. mjosi* and *S. stenops*, are recovered as sister taxa (Fig. 5; File S1 [figs S2–S8]). The genus *Hesperosaurus* was proposed as a subjective junior synonym of *Stegosaurus* (Maidment et al. 2008, 2015). However, recent studies regard it as a separate genus (e.g., Carpenter 2010; Raven and Maidment 2017; Maidment et al. 2018), as originally proposed by Carpenter et al. (2001). Further osteological

descriptions based on several relatively complete specimens housed in Sauriermuseum Aathal (Siber and Mockli 2009) may shed light on the stegosaurian taxonomy of the Morrison Formation.

The neostegosaurs *Al. longispinus* (Kimmeridgian–Tithonian, Morrison Formation, USA), *K. aethiopicus* (Kimmeridgian–Tithonian, Tendaguru Formation, Tanzania), *Th. atlasicus* (Bathonian–?Callovian, El Mers III Formation, Morocco), *Ad. boulahfa* (Bathonian, ?El Mers II Formation, Morocco), and *D. armatus* (Kimmeridgian–Tithonian, Kimmeridge Clay, Argiles d’ Octeville, Lourinhã, and Villar del Arzobispo Formations, UK, France, Portugal, and Spain) are included in Dacentrurinae (Fig. 5; File S1 [figs S2–S8]). This clade is supported by a single synapomorphy: presence of two pairs of long terminal caudal dermal spines (char. 114.1) (File S1 [table S3]). These phylogenetic analyses (Fig. 5; File S1 [figs S2–S8]) are the first to include *Al. longispinus* and *K. aethiopicus* within Dacentrurinae. Moreover, they also clearly distinguish the species *Al. longispinus* and *D. armatus*, thus supporting the separation of the genera *Alcovasaurus* Galton and Carpenter 2016 and *Dacentrurus* (Sánchez-Fenollosa et al. 2025; contra Costa and Mateus 2019). In recent phylogenetic analyses, *Al. longispinus* has been recovered as an early-diverging thyreophoran outside Eurypoda (Raven and Maidment 2017) or as an early-diverging stegosaurid (e.g., Maidment et al. 2020; Jia et al. 2024; Li et al. 2024a; Zafaty et al. 2024). Raven and Maidment (2017) erroneously coded several characters of *Al. longispinus* that explain the early-diverging position: (1) the presence of eight cervical vertebrae (char. 5 in Raven and Maidment 2017), (2) an acetabular length of ilium/dorsoventral height of pubic peduncle of ilium ratio of 1.8 (char. 18 in Raven and Maidment 2017), and (3) the presence of elongated posterior caudal vertebrae (char. 74 in Raven and Maidment 2017). According to Galton and Carpenter (2016), *Al. longispinus* preserves only one (or possibly two) cervical vertebrae, the ilium is extremely badly figured (field photos) and possibly broken, and the posterior caudal vertebrae are short. These errors were retained in later analyses based on the same data matrix (e.g., Maidment et al. 2020; Jia et al. 2024; Li et al. 2024a; Zafaty et al. 2024).

*Th. atlasicus*, *Ad. boulahfa*, and *D. armatus* are recovered as closely related taxa (Fig. 5; File S1 [figs S2–S8]). The clade that includes only these species is supported by a single synapomorphy: dorsal centra wider than long (char. 50.1). This character is also observed in several stegosaurian specimens from the Upper Jurassic and Berriasian (Lower Cretaceous) of Europe (e.g., Pereda-Suñer et al. 2003; Cobos et al. 2010; Company et al. 2010; Allain et al. 2022).

Regarding ichnological evidence, tracks with stegosaurian affinities like the ichnogenus *Deltapodus* Whyte & Romano, 1994 have been reported from the Middle Jurassic of Europe (Whyte and Romano 2001), the Upper Jurassic–Berriasian of almost world-wide (e.g., Cobos et al. 2010; Belvedere and Mietto 2010; Mateus et al. 2011; Pascual et al. 2012; Zhang et al. 2012; Lockley et al. 2017; Castanera et al. 2024), the Lower Cretaceous of

China (Xing et al. 2013, 2021), and the Upper Cretaceous of India (Mohabey 1986). Moreover, tracks with thyreophoran (probably stegosaurian) affinities such as the ichnogenera *Shenmuichnus* Li et al., 2012 and *Moyenisauropus* Ellenberg 1974 have been reported from at least the Early Jurassic of Europe and Asia (Gierliński 1999; Li et al. 2012; Xing et al. 2016; Figueiredo et al. 2024). Therefore, the ichnological evidence appears consistent with the osteological record and the origin and evolutionary history of stegosaurs suggested here.

## Conclusions

A new stegosaurian specimen has been studied here, comprising both cranial and postcranial fossils (Villar del Arzobispo Formation, upper Kimmeridgian–Tithonian). It preserves the most complete stegosaurian skull discovered in Europe. The cranial material consists of the posterior half of the skull roof, including a fragment of the right prefrontal, both frontals, both postorbitals, both squamosals, the parietal, the supraoccipital, and a possible fragment of the left paroccipital process. Among the postcranial material, a mid cervical vertebra (MAP-9030) has been described and systematically studied in detail, revealing three autapomorphies of *D. armatus*. Based on this evidence, this new stegosaurian specimen can be confidently referred to this species. Furthermore, the diagnosis of *D. armatus* has been updated with the identification of a new cranial autapomorphy: a posteroventrally oriented supraoccipital with an angle greater than 90° with the dorsal plane of the skull roof.

This discovery, along with other previous ones, makes *D. armatus* one of the stegosaurs with a better-known skull anatomy. The osteological and comparative study sheds light on the character evolution and reveals that *D. armatus* exhibits apomorphic characters more similar to neostegosaurs such as *S. stenops* than to huayangosaurids such as *H. taibaii*. Thus, the Iberian cranial material is essential for understanding skull evolution in stegosaurs.

In accordance with the PhyloCode, stegosaurian phylogenetic nomenclature has been revised to facilitate communication, discussion, and comparison between stegosaurian evolutionary hypotheses. This revision includes the formalization of two pre-existing clade names (Stegosaurinae and Dacentrurinae) and the introduction of a new clade name (Neostegosauria).

A new data matrix (115 morphological characters and 30 Operational Taxonomic Units), comprising all stegosaurian valid taxa, has been analysed applying Maximum Parsimony to infer phylogenetic relationships.

Phylogenetic analyses suggest that Stegosauria is divided into two major clades: Huayangosauridae and Stegosauridae. *I. mollensis* is recovered as a stegosaur within Huayangosauridae, which also includes several Asian stegosaurs from Middle to Late Jurassic (*H. taibaii*, *B. primitivus*, *Ba. baojiensis*, and *G. sichuanensis*). *M. expectabilis* is recovered as a huayangosaurid or an

early-diverging stegosaurid, suggesting that a lineage of these persisted in Asia until at least the late Early Cretaceous. Stegosauridae includes *C. jiangbeiensis*, *T. multispinus* and *P. africanus* as sister taxa, and Neostegosauria (Stegosaurinae + Dacentrurinae). Some variations in the composition of Huayangosauridae and Stegosauridae occur when applying analyses using IW parsimony with low concavity constant values ( $k = 3$ ).

Stegosaurinae is divided into two distinct lineages: one including the Qiketai stegosaur, *Lo. priscus*, *He. mjosi*, and *S. stenops*, and another comprising *J. junggarensis*, *W. homheni*, *Ya. ultimus*, and the Zhongpu stegosaur. This suggests that *Wuerhosaurus* and *Stegosaurus* are separate genera, and that a taxonomic re-evaluation of Early Cretaceous stegosaurs from China is necessary. Phylogenetic analyses also indicate that *Al. longispinus* and *K. aethiopicus* are dacentrurines, and that *D. armatus* is closely related to *Th. atlasicus* and *Ad. bouldahfa* from the Middle Jurassic of Morocco.

The chronogram produced in this study, along with the available evidence, supports that stegosaurs appeared in the Early Jurassic, diversified rapidly during the Middle Jurassic, became important constituents of ecosystems at least in the Late Jurassic, and declined in the Early Cretaceous.

The low support values for most stegosaurian clades in all phylogenetic analyses (including this study) are likely because most stegosaurian taxa are represented by a single partial skeleton and highly incomplete material. Further fieldwork, new fossil discoveries, and comprehensive taxonomic revisions are needed to improve the understanding of stegosaurian evolution.

## Acknowledgements

We are grateful to the colleagues from the Fundación Conjunto Paleontológico de Teruel-Dinópolis (Teruel, Spain) for their support. We thank the Riodeva Town Council and especially M. Tomás for notifying the FCPT-D about the discovery of the first fossils at the Están de Colón site. We acknowledge B. Holgado for the information supplied and J.I. Kirkland for providing numerous photos of thyreophorans. We thank D. Schwarz (Museum für Naturkunde), C.A. Tomás (Museu da Lourinhã), S. Mateus (Dino Parque Lourinhã), B. Poza (Museo de Ciencias Naturales de Valencia), A. Galobart and J.M. Robles (Institut Català de Paleontologia Miquel Crusafont), and S.C.R. Maidment and M.E.H. Jones (Natural History Museum), for access to specimens under their care. We appreciate S.C.R. Maidment and P. Barrett for sharing the 3D models of the postcranial skeleton of ‘Sophie’, and J.C. Mallon for openly sharing (via MorphoSource) the 3D model of the skull of *Ankylosaurus magniventris* (CMN 8880). We also thank S.C.R. Maidment for discussions on stegosaurian phylogeny. We appreciate S. Hartman and I. Fein for openly sharing (via PhyloPic) the thyreophoran silhouettes. TNT was made available by the Willi Hennig Society. We are grateful for the valuable comments and suggestions made by the chief editor Uwe Fritz and the referees Kenneth Carpenter and Omar Rafael Regalado Fernández, which have been very useful in improving this manuscript.

This research was funded by the Gobierno de Aragón through the research group E04\_23R FOCONTUR, the Ministerio de Ciencia, In-

novación y Universidades (Gobierno de España) through the Unidad de Paleontología de Teruel, and the Instituto Aragonés de Fomento.

Author contributions were as follows: Conceptualization: S.S.-F. and A.C.; Resources: S.S.-F. and A.C.; Investigation: S.S.-F. and A.C.; Software: S.S.-F.; Data Curation: S.S.-F.; Methodology: S.S.-F.; Formal Analysis: S.S.-F.; Validation: A.C.; Writing – Original Draft: S.S.-F.; Writing – Review and Editing: S.S.-F. and A.C.; Visualization: S.S.-F.; Supervision: A.C.; Project Administration: A.C.; Funding Acquisition: A.C.

## References

- Allain R, Vullo R, Rozada L, Anquetin J, Bourgeois R, Goedert J, Lasseron M, Martin JE, Pérez-García A, Peyre de Fabrègues C, Royo-Torres R, Augier D, Bailly G, Cazes L, Despres Y, Gailliègue A, Gomez B, Goussard F, Lenglet T, Vacant R, Tournepiche JF (2022) Vertebrate paleobiodiversity of the Early Cretaceous (Berriasian) Angéac-Charente Lagerstätte (southwestern France): Implications for continental faunal turnover at the J/K boundary. *Geodiversitas* 25: 683–752. <https://doi.org/10.5252/geodiversitas2022v44a25>
- Arbour VM, Currie PJ (2013) *Euoplocephalus tutus* and the diversity of ankylosaurid dinosaurs in the Late Cretaceous of Alberta, Canada, and Montana, USA. *PLOS One* 8: e62421. <https://doi.org/10.1371/journal.pone.0062421>
- Arbour VM, Mallon JC (2017) Unusual cranial and postcranial anatomy in the archetypal ankylosaur *Ankylosaurus magniventris*. *Facets* 2: 764–794. <https://doi.org/10.1139/facets-2017-0063>
- Bapst DW (2012) Paleotree: An R package for paleontological and phylogenetic analyses of evolution. *Methods in Ecology and Evolution* 3: 803–807.
- Baron MG, Norman DB, Barrett PM (2017) Postcranial anatomy of *Lesothosaurus diagnosticus* (Dinosauria: Ornithischia) from the Lower Jurassic of southern Africa: Implications for basal ornithischian taxonomy and systematics. *Zoological Journal of the Linnean Society* 179: 125–168. <https://doi.org/10.1111/zoj.12434>
- Belvedere M, Mietto P (2010) First evidence of stegosaurian *Deltapodus* footprints in North Africa (Iouaridène Formation, Upper Jurassic, Morocco). *Palaeontology* 53: 233–240. <https://doi.org/10.1111/j.1475-4983.2009.00928.x>
- Billon-Bruyat JP, Mazin JM, Pouech J (2010) A stegosaur tooth (Dinosauria, Ornithischia) from the Early Cretaceous of southwestern France. *Swiss Journal of Geosciences* 103: 143–153. <https://doi.org/10.1007/s00015-010-0028-y>
- Boyd CA (2015) The systematic relationships and biogeographic history of ornithischian dinosaurs. *PeerJ* 3: e1523. <https://doi.org/10.7717/peerj.1523>
- Breedon III BT, Raven TJ, Butler RJ, Rowe TB, Maidment SCR (2021) The anatomy and palaeobiology of the early armoured dinosaur *Scutellosaurus lawleri* (Ornithischia: Thyreophora) from the Kayenta Formation (Lower Jurassic) of Arizona. *Royal Society Open Science* 8: 201676. <https://doi.org/10.1098/rsos.201676>
- Breedon III BT, Rowe TB (2020) New specimens of *Scutellosaurus lawleri* Colbert, 1981, from the Lower Jurassic Kayenta Formation in Arizona elucidate the early evolution of thyreophoran dinosaurs. *Journal of Vertebrate Paleontology* 40: e1791894. <https://doi.org/10.1080/02724634.2020.1791894>
- Brusatte SL (2011) Calculating the Tempo of Morphological Evolution: Rates of Discrete Character Change in a Phylogenetic Context. In: Elewa AMT (Ed.) *Computational Paleontology*. Springer, Berlin, 53–74.
- Brusatte SL, Benton MJ, Ruta M, Lloyd GT (2008) Superiority, competition, and opportunism in the evolutionary radiation of dinosaurs. *Science* 321: 1485–1488. <https://doi.org/10.1126/science.1161833>
- Butler RJ (2005) The ‘fabrosaurid’ ornithischian dinosaurs of the Upper Elliot Formation (Lower Jurassic) of South Africa and Lesotho. *Zoological Journal of the Linnean Society* 145: 175–218. <https://doi.org/10.1111/j.1096-3642.2005.00182.x>
- Butler RJ, Upchurch P, Norman DB (2008) The phylogeny of the ornithischian dinosaurs. *Journal of Systematic Palaeontology* 6: 1–40. <https://doi.org/10.1017/S1477201907002271>
- Campos-Soto S, Benito MI, Cobos A, Caus E, Quijada IE, Suarez-González P, Mas R, Royo-Torres R, Alcalá L (2019) Revisiting the age and palaeoenvironments of the Upper Jurassic-Lower Cretaceous? dinosaur-bearing sedimentary record of eastern Spain: Implications for Iberian palaeogeography. *Journal of Iberian Geology* 45: 471–510. <https://doi.org/10.1007/s41513-019-00106-y>
- Campos-Soto S, Benito MI, Mas R, Caus E, Cobos A, Suarez-González P, Quijada IE (2016) Revisiting the Late Jurassic–Early Cretaceous of the NW South Iberian Basin: New ages and sedimentary environments. *Journal of Iberian Geology* 42: 69–94. [https://doi.org/10.5209/rev\\_JIGE.2016.v42.n1.51920](https://doi.org/10.5209/rev_JIGE.2016.v42.n1.51920)
- Campos-Soto S, Benito MI, Moutney NP, Plink-Björklund P, Quijada IE, Suarez-González P, Cobos A (2021) Where humid and arid meet: Sedimentology of coastal siliciclastic successions deposited in apparently contrasting climates. *Sedimentology* 69: 975–1027. <https://doi.org/10.1111/sed.12958>
- Campos-Soto S, Cobos A, Caus E, Benito MI, Fernández-Labrador L, Suarez-González P, Quijada IE, Mas R, Royo-Torres R, Alcalá L (2017) Jurassic Coastal Park: A great diversity of palaeoenvironments for the dinosaurs of the Villar del Arzobispo Formation (Teruel, eastern Spain). *Palaeogeography, Palaeoclimatology, Palaeoecology* 485: 154e177. <https://doi.org/10.1016/j.palaeo.2017.06.010>
- Carpenter K (2004) Redescription of *Ankylosaurus magniventris* Brown 1908 (Ankylosauridae) from the Upper Cretaceous of the Western Interior of North America. *Canadian Journal of Earth Sciences* 41: 961–986. <https://doi.org/10.1139/e04-043>
- Carpenter K (2010) Species concept in North American stegosaurs. *Swiss Journal of Geosciences* 103: 155–162. <https://doi.org/10.1007/s00015-010-0020-6>
- Carpenter K, Miles CA, Cloward K (1998) Skull of a Jurassic ankylosaur (Dinosauria). *Nature* 393: 782–783. <https://doi.org/10.1038/31684>
- Carpenter K, Miles CA, Cloward K (2001) New primitive Stegosaur from the Morrison Formation, Wyoming. In: Carpenter K (Ed.) *The Armored Dinosaurs*. Indiana University Press, Bloomington, IN, 55–75.
- Casanovas-Cladellas ML, Santafé-Llopis JV, Santisteban C (1995) *Dacentrurus armatus* (Stegosauria, Dinosauria) del Cretácico Inferior de Los Serranos (Valencia, España). *Revista Española de Paleontología* 10: 273–83.
- Castanera D, Mampel L, Cobos A (2024) The complexity of tracking stegosaurs and their gregarious behavior. *Scientific Reports* 14. <https://doi.org/10.1038/s41598-024-64298-9>
- Cobos A, Royo-Torres R, Alcalá L (2008) Presencia del estegosaurio *Dacentrurus* en Riodeva. In: Ruiz-Omeñaca JI, Piñuela L, García-Ramos JC (Eds) *XXIV Jornadas de la Sociedad Española de Paleontología*, Colunga (Spain), 89–90.
- Cobos A, Royo-Torres R, Luque L, Alcalá L, Mampel L (2010) An Iberian stegosaurs paradise: The Villar del Arzobispo Formation (Tithonian–Berriasian) in Teruel (Spain). *Palaeogeography Palaeo-*

- climatology Palaeoecology 293: 223–236. <https://doi.org/10.1016/j.palaeo.2010.05.024>
- Colbert EH (1981) A primitive ornithischian dinosaur from the Kayenta Formation of Arizona. Museum of Northern Arizona Press 53: 1–65.
- Company J, Pereda-Suberbiola X, Ruiz-Omeñaca JI (2010) New stegosaurian (Ornithischia, Thyreophora) remains from Jurassic–Cretaceous transition beds of Valencia province (Southwestern Iberian Range, Spain). Journal of Iberian Geology 36: 243–252. [https://doi.org/10.5209/rev\\_JIGE.2010.v36.n2.10](https://doi.org/10.5209/rev_JIGE.2010.v36.n2.10)
- Congreve CR, Lamsdell JC (2016) Implied weighting and its utility in palaeontological datasets: A study using modelled phylogenetic matrices. Palaeontology 59: 447–462. <https://doi.org/10.1111/pala.12236>
- Costa F, Mateus O (2019) Dacentrurine stegosaurs (Dinosauria): A new specimen of *Miragaia longicollum* from the Late Jurassic of Portugal resolves taxonomical validity and shows the occurrence of the clade in North America. PLOS One 14: e0224263. <https://doi.org/10.1371/journal.pone.0224263>
- Czerkas S (1999) The beaked jaw of stegosaurs and their implications for other ornithischians. In: Gillette DD (Ed.) Vertebrate Paleontology in Utah. Miscellaneous Publications of Utah Geological Survey, Utah Geological and Mineral Survey, Salt Lake City, UT, 143–150.
- Dai H, Ning L, Maidment SCR, Guangbiao W, Yuxuan Z, Xufeng H, Qingyu M, Xunqian W, Haiqian H, Guangzhao P (2022) New stegosaurs from the Middle Jurassic Lower Member of the Shaximiao Formation of Chongqing, China. Journal of Vertebrate Paleontology 41: e1995737. <https://doi.org/10.1080/02724634.2021.1995737>
- Davies W (1876) On the exhumation and development of a large reptile (*Omosaurus armatus*, owen), from the Kimmeridge Clay, Swindon, Wilts. Geological Magazine 33: 193–197.
- Delvene G, Munt M, Royo-Torres R, Cobos A, Alcalá L (2013) Late Jurassic–Early Cretaceous freshwater bivalves from *Turiasaurus riodevensis* bearing strata of Teruel (Spain). Spanish Journal of Palaeontology 28: 161–172. <https://doi.org/10.7203/sjp.28.2.17850>
- DeSantis LRG, Sharp AC, Schubert BW, Colbert MW, Wallace SC, Grine FE (2020) Clarifying relationships between cranial form and function in tapirs, with implications for the dietary ecology of early hominins. Scientific Reports 10: 8809. <https://doi.org/10.1038/s41598-020-65586-w>
- Dieudonné PE, Cruzado-Caballero P, Godefroit P, Tortosa T (2021) A new phylogeny of cerapodan dinosaurs. Historical Biology 33: 2335–2355. <https://doi.org/10.1080/08912963.2020.1793979>
- Dong Z (1973) Dinosaurs from Wuerho. Institute of Paleontology and Paleoanthropology Memoir 11: 45–52.
- Dong Z (1990) Stegosaurs of Asia. In: Carpenter K, Currie PJ (Eds) Dinosaur systematics, approaches and perspectives. Cambridge University Press, Cambridge, 255–268.
- Dong Z (1993) A new species of stegosaur (Dinosauria) from the Ordos Basin, Inner Mongolia, People's Republic of China. Canadian Journal of Earth Sciences 30: 2174–2176.
- Dong Z, Li X, Zhou S, Chang Y (1977) On the stegosaurian remain from Zigong (Tzekung), Zsechuan Province. Vertebrata Palasiatica 15: 307–315 [in Chinese, with English abstract].
- Dong Z, Tang Z, Zhou S (1982) Note on the new Mid-Jurassic stegosaur from Sichuan Basin, China. Vertebrata Palasiatica 20: 84–88 [in Chinese].
- Dong Z, Zhou S, Chang Y (1983) Dinosaurs from the Jurassic of Sichuan. Palaeontologica Sinica 162: 1–136 (Translated by W Downs).
- Escaso F (2014) Historia evolutiva de los Ornithischia (Dinosauria) del Jurásico Superior de Portugal. PhD Thesis, Universidad Autónoma de Madrid, Madrid, 350 pp.
- Escaso F, Ortega F, Dantas P, Malafaia E, Pimentel NL, Pereda-Suberbiola X, Sanz JL, Kullberg JC, Kullberg MC, Barriga F (2007a) New evidence of shared dinosaur across Upper Jurassic Proto-North Atlantic: *Stegosaurus* from Portugal. Naturwissenschaften 94: 367–374. <https://doi.org/10.1007/s00114-006-0209-8>
- Escaso F, Ortega F, Dantas P, Malafaia E, Silva B, Sanz JL (2007b) Elementos postcraneales de *Dacentrurus* (Dinosauria: Stegosauria) del Jurásico Superior de Moçafaneira (Torres Vedras, Portugal). In: Cambra-Moo O, Martínez-Pérez C, Chamero B, Escaso F, Esteban-Trivigno, Marugán-Lobón J (Eds) Cantera Paleontológica. Diputación Provincial de Cuenca, Cuenca, 157–172.
- Ezcurra MD (2024) Exploring the effects of weighting against homoplasy in genealogies of palaeontological phylogenetic matrices. Cladistics 40: 242–281. <https://doi.org/10.1111/cla.12581>
- Figueiredo SD, Carvalho CN, Cunha PP, Duarte LV, Fonseca A, Monteiro C, Forte J (2024) The first dinosaurs in Iberia: A new dinosaur tracksite from the Sinemurian (Lower Jurassic) of Portugal. Historical Biology 36: 2339–2352. <https://doi.org/10.1080/08912963.2023.2256751>
- Figueirido B, Tseng ZJ, Serrano-Alarcón FJ, Martín-Serra A, Pastor JF (2014) Three-dimensional computer simulations of feeding behaviour in red and giant pandas relate skull biomechanics with dietary niche partitioning. Biology Letters 10: 20140196. <https://doi.org/10.1098/rsbl.2014.0196>
- Fonseca AO, Reid IJ, Venner A, Duncan RJ, Garcia MS, Müller RT (2024) A comprehensive phylogenetic analysis on early ornithischian evolution. Journal of Systematic Palaeontology, 22: 2346577. <https://doi.org/10.1080/14772019.2024.2346577>
- Galton PM (1978) Fabrosauridae, the basal family of ornithischian dinosaurs (Reptilia: Ornithopoda). Paläontologische Zeitschrift 52: 138–159.
- Galton PM (1981) *Craterosaurus pottonensis* Seeley, a stegosaurian dinosaur from the Lower Cretaceous of England, and a review of Cretaceous stegosaurs. Neues Jahrbuch für Geologie und Paläontologie, Abhandlungen 161: 28–46.
- Galton PM (1982) The postcranial Anatomy of stegosaurian dinosaur *Kentrosaurus* from the Upper Jurassic of Tanzania, East Africa. Geologica et Palaeontologica 15: 139–160.
- Galton PM (1985) British plated dinosaurs (Ornithischia, Stegosauridae). Journal of Vertebrate Paleontology 5: 211–254. <https://doi.org/10.1080/02724634.1985.10011859>
- Galton PM (1988) Skull bones and endocranial casts of stegosaurian dinosaur *Kentrosaurus* Hennig, 1915 from Upper Jurassic of Tanzania, East Africa. Geologica et Palaeontologica 22: 123–143.
- Galton PM (1990) A partial skeleton of the stegosaurian dinosaur *Lexovisaurus* from the uppermost Lower Callovian (Middle Jurassic) of Normandy, France. Geologica et Palaeontologica 24: 185–199.
- Galton PM (1991) Postcranial remains of stegosaurian dinosaur *Dacentrurus* from Upper Jurassic of France and Portugal. Geologica et Palaeontologica 25: 299–327.
- Galton PM (2016) Notes on plated dinosaurs (Ornithischia: Stegosauria), mostly on dermal armor from Middle and Upper Jurassic of England (also France, Iberia), with a revised diagnosis for *Loricatosaurus priscus* (Callovian, England). Neues Jahrbuch für Geologie und Paläontologie, Abhandlungen 282: 1–25. <https://doi.org/10.1127/njgpa/2016/0603>
- Galton PM, Carpenter K (2016) The plated dinosaur *Stegosaurus longispinus* Gilmore, 1914 (Dinosauria: Ornithischia; Upper Jurassic, western USA), type species of *Alcovasaurus* n. gen. Neues Jahrbuch

- buch für Geologie und Paläontologie, Abhandlungen 279: 185–208. <https://doi.org/10.1127/njgpa/2016/0551>
- Galton PM, Coombs WP (1981) A stegosaurian dinosaur from the Lower Cretaceous of South Africa. *Geobios* 14: 299–309.
- Galton PM, Upchurch P (2004) Stegosauria. In: Weishampel DB, Dodson P, Osmólska H (Eds) *The Dinosauria*, Second Edition. University of California Press, Oakland, CA, 343–362.
- Gierliński G (1999) Tracks of a large thyreophoran dinosaur from the Early Jurassic of Poland. *Acta Paleontologica Polonica* 44: 231–234.
- Gilmore CW (1914) Osteology of the armored dinosaurian in the United States National Museum, with special reference to the genus *Stegosaurus*. *United States National Museum Bulletin* 89: 1–143.
- Goloboff PA, Morales ME (2023) TNT version 1.6, with a graphical interface for MacOs and Linux, including new routines in parallel. *Cladistics* 39: 144–153. <https://doi.org/10.1111/cla.12524>
- Goloboff PA, Szumik CA (2015) Identifying unstable taxa: Efficient implementation of triplet-based measures of stability, and comparison with Phyutility and RogueNaRok. *Molecular Phylogenetics and Evolution* 88: 93–104. <https://doi.org/10.1016/j.ympev.2015.04.003>
- Goloboff PA, Torres A, Arias JS (2018) Weighted parsimony outperforms other methods of phylogenetic inference under models appropriate for morphology. *Cladistics* 34: 407–437. <https://doi.org/10.1111/cla.12205>
- Han F, Forster CA, Xu X, Clark JM (2018) Postcranial anatomy of *Yinlong downsi* (Dinosauria: Ceratopsia) from the Upper Jurassic Shishugou Formation of China and the phylogeny of basal ornithischians. *Journal of Systematic Palaeontology* 16: 1159–1187. <https://doi.org/10.1080/14772019.2017.1369185>
- Hao B, Zhang Q, Peng G, Ye Y, You H (2018) Redescription of *Gigantospinosaurus sichuanensis* (Dinosauria, Stegosauria) from the Late Jurassic of Sichuan, Southwestern China. *Acta Geologica Sinica*, 92: 431–441. <https://doi.org/10.1111/1755-6724.13535>
- Haubold H (1990) Ein neuer Dinosaurier (Ornithischia, Thyreophora) aus dem unteren Jura des nördlichen Mitteleuropa. *Revue de Paléobiologie* 9: 149–177.
- Hennig E (1915a). *Kentrosaurus aethiopicus*, der Stegosauride des Tendaguru. *Sitzungsberichte der Gesellschaft naturforschender Freunde zu Berlin*: 219–247.
- Hennig E (1916) Zweite Mitteilung über den Stegosauriden vom Tendaguru. *Sitzungsberichte der Gesellschaft naturforschender Freunde zu Berlin*: 175–182.
- Hennig E (1925) *Kentrurosaurus aethiopicus*. Die Stegosaurier-Funde vom Tendaguru, Deutsch-Ostafrika. *Palaeontographica* 7: 101–254.
- International Commission on Zoological Nomenclature (2013) Opinion 2320 (Case 3536). *Stegosaurus* Marsh, 1877 (Dinosauria, Ornithischia): Type species replaced with *Stegosaurus stenops* Marsh, 1887. *Bulletin of Zoological Nomenclature* 70: 129–130.
- Jia C, Foster CA, Xu X, Clark, JM (2007) The first stegosaur (Dinosauria, Ornithischia) from the Upper Jurassic Shishugou Formation of Xinjiang, China. *Acta Geologica Sinica* 81: 351–356. <https://doi.org/10.1111/j.1755-6724.2007.tb00959.x>
- Jia L, Li N, Dong L, Shi J, Kang Z, Wang S, Wu S, You H (2024) A new stegosaur from the late Early Cretaceous of Zuoyun, Shanxi Province, China. *Historical Biology*. <https://doi.org/10.1080/08912963.2024.2308214>
- Kirkland JI, Alcalá L, Loewen MA, Espílez E, Mampel L, Wiersma JP (2013) The basal nodosaurid ankylosaur *Europelta carbonensis* n. gen., n. sp. from the Lower Cretaceous (Lower Albian) Escucha Formation of northeastern Spain. *PLOS One* 8: e80405. <https://doi.org/10.1371/journal.pone.0080405>
- Langer MC, Novas FE, Bittencourt JS, Ezcurra MD, Gauthier JA (2020) *Dinosauria* R. Owen 1842 [M. C. Langer, F. E. Novas, J. S. Bittencourt, M. D. Ezcurra, and J. A. Gauthier], converted clade name. In: de Queiroz K, Cantino PD, Gauthier JA (Eds) *Phylogonyms: A Companion to the PhyloCode*. CRC Press, Boca Raton, 1209–1217.
- Leahey LG, Molnar RE, Carpenter K, Witmer LM, Salisbury SW (2015) Cranial osteology of the ankylosaurian dinosaur formerly known as *Minmi* sp. (Ornithischia: Thyreophora) from the Lower Cretaceous Allaru Mudstone of Richmond, Queensland, Australia. *PeerJ* 3: e1475. <https://doi.org/10.7717/peerj.1475>
- Li JJ, Lockley MG, Zhang YU, Hu S, Matsukawa M, Bai, ZQ (2012) An important ornithischian tracksite in the Early Jurassic of the Shenmu region, Shaanxi, China. *Acta Geologica Sinica* 86: 1–10. <https://doi.org/10.1111/j.1755-6724.2012.00606.x>
- Li N, Chen G, Mateus O, Jiang T, Xie Y, Li D, You H, Peng G (2024a) A new stegosaur (Dinosauria: Ornithischia) from the Upper Jurassic Qigu Formation of Xinjiang, China and a revision on Chinese stegosaurs phylogeny. *bioRxiv*. <https://doi.org/10.1101/2024.09.29.615678>
- Li N, Li D, Peng G, You H (2024c) The first stegosaurian dinosaur from Gansu Province, China. *Cretaceous Research* 158: 105852. <https://doi.org/10.1016/j.cretres.2024.105852>
- Li N, Maidment SCR, Li D, You H, Peng G (2024b) A new stegosaur (Dinosauria: Ornithischia) from the Middle Jurassic of Gansu Province, China. *Scientific Reports* 14: 15241. <https://doi.org/10.1038/s41598-024-66280-x>
- Lockley MG, Gierliński G, Matthews N, Xing L, Foster J, Cart K (2017) New dinosaur track occurrences from the Upper Jurassic Salt Wash Member (Morrison Formation) of southeastern Utah: Implications for thyreophoran trackmaker distribution and diversity. *Palaeogeography Palaeoclimatology Palaeoecology* 470: 116–121. <https://doi.org/10.1016/j.palaeo.2016.12.047>
- Maddison WP, Maddison DR (2023) Mesquite: A modular system for evolutionary analysis. Version 3.81. <http://www.mesquiteproject.org> [accessed 2 September 2024].
- Madzia D, Arbour VM, Boyd CA, Farke AA, Cruzado-Caballero P, Evans DC (2021) The phylogenetic nomenclature of ornithischian dinosaurs. *PeerJ* 9: e12362. <https://doi.org/10.7717/peerj.12362>
- Maidment SCR (2010) Stegosauria: A historical review of the body fossil record and phylogenetic relationships. *Swiss Journal of Geosciences* 103: 199–210. <https://doi.org/10.1007/s00015-010-0023-3>
- Maidment SCR, Brassey C, Barrett PM (2015) The postcranial skeleton of an exceptionally complete individual of the plated dinosaur *Stegosaurus stenops* (Dinosauria: Thyreophora) from the Upper Jurassic Morrison Formation of Wyoming, U.S.A. *PLOS One* 10: e0138352. <https://doi.org/10.1371/journal.pone.0138352>
- Maidment SCR, Norman DB, Barrett PM, Upchurch P (2008) Systematics and phylogeny of Stegosauria (Dinosauria: Ornithischia). *Journal of Systematic Palaeontology* 6: 367–407. <https://doi.org/10.1017/S1477201908002459>
- Maidment SCR, Porro L (2010) Homology of the palpebral and origin of supraorbital ossifications in ornithischian dinosaurs. *Lethaia* 43: 95–111. <https://doi.org/10.1111/j.1502-3931.2009.00172.x>
- Maidment SCR, Raven TJ, Ouarhache D, Barrett PM (2020) North Africa's first stegosaur: Implications for Gondwanan thyreophoran dinosaur diversity. *Gondwana Research* 77: 82–97. <https://doi.org/10.1016/j.gr.2019.07.007>

- Maidment SCR, Wei G (2006) A review of the Late Jurassic stegosaurs (Dinosauria, Stegosauria) from the People's Republic of China. *Geological Magazine* 143: 621–634. <https://doi.org/10.1017/S0016756806002500>
- Maidment SCR, Wei G, Norman DB (2006) Re-description of the postcranial skeleton of the middle Jurassic stegosaur *Huayangosaurus taibaii*. *Journal of Vertebrate Paleontology* 26: 944–956. [https://doi.org/10.1671/0272-4634\(2006\)26\[944:ROTPSO\]2.0.CO;2](https://doi.org/10.1671/0272-4634(2006)26[944:ROTPSO]2.0.CO;2)
- Maidment SCR, Woodruff DC, Horner JR (2018) A new specimen of the ornithischian dinosaur *Hesperosaurus mjosi* from the Upper Jurassic Morrison Formation of Montana, USA, and implications for growth and size in Morrison stegosaurs. *Journal of Vertebrate Paleontology* 38: e1406366. <https://doi.org/10.1080/02724634.2017.1406366>
- Mallison H (2010) CAD assessment of the posture and range of motion of *Kentrosaurus aethiopicus* Hennig 1915. *Swiss Journal of Geosciences* 103: 211–233. <https://doi.org/10.1007/s00015-010-0024-2>
- Marsh OC (1877) A new order of extinct Reptilia (Stegosauria) from the Jurassic of the Rocky Mountains. *American Journal of Science* 3<sup>rd</sup> series 14: 513–514.
- Martill DM, Earland S, Naish D (2006) Dinosaurs in marine strata: Evidence from the British Jurassic, including a review of the allochthonous vertebrate assemblage from the marina Kimmeridge Clay Formation (Upper Jurassic) of Great Britain. In: *Colectivo Arqueológico-Paleontológico Salense* (Ed.) *Actas de las III Jornadas sobre Dinosaurios y su Entorno*, Salas de los Infantes (Spain), 1–31.
- Mas R, Alonso A, Meléndez N (1984) La Formación Villar del Arzobispo: un ejemplo de llanuras de mareas siliciclásticas asociadas a plataformas carbonatadas. *Jurásico terminal*. (NE de Valencia y E de Cuenca). *Publicaciones de Geología de la Universidad Autónoma de Barcelona* 20: 175–88.
- Mas R, García A, Salas R, Meléndez A, Alonso A, Aurell M, Bádenas B, Benito MI, Carenas B, García-Hidalgo JF, Gil J, Segura M (2004) Segunda fase de rifting: Jurásico Superior-Cretácico Inferior. In: Vera JA (Ed) *Geología de España*. SGE–IGME, Madrid, 503–510.
- Mateus O, Maidment SCR, Christiansen NA (2009) A new long-necked “sauropod mimic” stegosaur and the evolution of the plated dinosaurs. *Proceedings of the Royal Society Biological Sciences* 276: 1815–1821. <https://doi.org/10.1098/rspb.2008.1909>
- Mateus O, Milàn J, Romano M, Whyte MA (2011) New finds of stegosaur tracks from the Upper Jurassic Lourinhã Formation, Portugal. *Acta Palaeontologica Polonica* 56: 651–658. <https://doi.org/10.4202/app.2009.0055>
- Mohabey DM (1986) Note on dinosaur footprint from Kheda district. Gujarat. *Journal of the Geological Society of India* 27: 456–459.
- Nopcsa F (1911b) *Omosaurus lennieri*, un nouveau dinosaurien du Cap de la Hève. *Bulletin de la Société Géologique de Normandie* 30: 23–42.
- Norman DB (2020a) *Scelidosaurus harrisonii* from the Early Jurassic of Dorset, England: cranial anatomy. *Zoological Journal of the Linnean Society* 188: 1–81. <https://doi.org/10.1093/zoolinnean/zlzo74>
- Norman DB (2020b) *Scelidosaurus harrisonii* from the Early Jurassic of Dorset, England: postcranial skeleton. *Zoological Journal of the Linnean Society* 189: 47–157. <https://doi.org/10.1093/zoolinnean/zlzo78>
- Norman DB (2020c) *Scelidosaurus harrisonii* from the Early Jurassic of Dorset, England: The dermal skeleton. *Zoological Journal of the Linnean Society* 190: 1–53. <https://doi.org/10.1093/zoolinnean/zlzo85>
- Norman DB (2021) *Scelidosaurus harrisonii* (Dinosauria: Ornithischia) from the Early Jurassic of Dorset, England: Biology and phylogenetic relationships. *Zoological Journal of the Linnean Society* 191: 1–86. <https://doi.org/10.1093/zoolinnean/zlzo061>
- Norman DB, Witmer LM, Weishampel DB (2004) Basal Thyreophora. In: Weishampel DB, Dodson P, Osmólska H (Eds) *The Dinosauria*, Second Edition. University of California Press, Oakland, CA, 335–342.
- O'Reilly JE, Puttick MN, Parry L, Tanner AR, Tarver JE, Fleming J, Pisani D, Donoghue PCJ (2016) Bayesian methods outperform parsimony but at the expense of precision in the estimation of phylogeny from discrete morphological data. *Biology Letters* 12: 20160081. <https://doi.org/10.1098/rsbl.2016.0081>
- Ostrom JH, McIntosh JS (1966) Stegosaur plates. In: Ostrom JH, McIntosh JS (Eds) *Marsh's Dinosaurs: The Collections from Como Bluff*. Yale University Press, New Haven, CT, 249–362.
- Owen R (1875) *Monographs of the fossil Reptilia of the Mesozoic Formations: Part II. Genera Bothriospondylus, Cetiosaurus, Omosaurus*. *Palaeontographical Society Monographs* 29: 15–94.
- Pacios D, Campos-Soto S, Suarez-González P, Benito MI, Cobos A, Caus E (2018) Revisión cartográfica y estratigráfica del Jurásico Superior–Cretácico Inferior de Vilella (Teruel). *Geogaceta* 63: 19–22.
- Pascual C, Canudo JI, Hernández N, Barco JL & Castanera D (2012) First record of stegosaur dinosaur tracks in the Lower Cretaceous (Berriasian) of Europe (Oncala group, Soria, Spain). *Geodiversitas* 34: 297–312. <https://doi.org/10.5252/g2012n2a4>
- Peng G, Ye Y, Gao Y, Shu C, Jiang S (2005) Jurassic dinosaur faunas in Zigong. *Sichuan Scientific and Technological Publishing House*: 214–247 [in Chinese, with English abstract].
- Pereda-Suberbiola X, Galton PM, Torcida F, Huerta P, Izquierdo LA, Montero D, Pérez G, Urién V (2003) First stegosaurian dinosaur remains from the Early Cretaceous of Burgos (Spain), with a review of Cretaceous stegosaurs. *Revista Española de Paleontología* 18: 143–150.
- Pereda-Suberbiola X, Galton PM, Mallison H, Novas F (2013) A plated dinosaur (Ornithischia, Stegosauria) from the Early Cretaceous of Argentina, South America: An evaluation. *Alcheringa: An Australasian Journal of Palaeontology* 37: 65–78. <https://doi.org/10.1080/03115518.2012.702531>
- Pol D, Escapa IH (2009) Unstable taxa in cladistic analysis: identification and the assessment of relevant characters. *Cladistics* 25: 515–527. <https://doi.org/10.1111/j.1096-0031.2009.00258.x>
- Porro LB, Witmer LM, Barrett PM (2015) Digital preparation and osteology of the skull of *Lesothosaurus diagnosticus* (Ornithischia: Dinosauria). *PeerJ* 3: e1494. <https://doi.org/10.7717/peerj.1494>
- R Core Team (2023) R: A Language and Environment for Statistical Computing. R Foundation for Statistical Computing, Vienna, Austria. <https://www.R-project.org> [accessed 2 September 2024].
- Rauhut OWM, Carballido JL, Diego P (2021) First osteological record of a stegosaur (Dinosauria, Ornithischia) from the Upper Jurassic of South America. *Journal of Vertebrate Paleontology* 40: e1862133. <https://doi.org/10.1080/02724634.2020.1862133>
- Raven TJ, Barrett PM, Joyce CB, Maidment SCR (2023) The phylogenetic relationships and evolutionary history of the armoured dinosaurs (Ornithischia: Thyreophora). *Journal of Systematic Palaeontology* 21: 2205433. <https://doi.org/10.1080/14772019.2023.2205433>
- Raven TJ, Maidment SCR (2017) A new phylogeny of Stegosauria (Dinosauria, Ornithischia). *Palaeontology* 60: 401–418. <https://doi.org/10.1111/pala.12291>
- Raven TJ, Maidment SCR (2018) The systematic position of the enigmatic thyreophoran dinosaur *Paranthodon africanus*, and the use of

- basal exemplifiers in phylogenetic analysis. *PeerJ* 6: e4529. <https://doi.org/10.7717/peerj.4529>
- Rosenbaum JN, Padian K (2000) New material of the basal thyreophoran *Scutellosaurus lawleri* from the Kayenta Formation (Lower Jurassic) of Arizona. *PaleoBios* 20: 13–23.
- Ruta M, Wagner PJ, Coates MI (2006) Evolutionary patterns in early tetrapods. I. Rapid initial diversification followed by decrease in rates of character change. *Proceedings of the Royal Society B* 273: 2107–2111. <https://doi.org/10.1098/rspb.2006.3577>
- Saitta ET (2015) Evidence for sexual dimorphism in the plated dinosaur *Stegosaurus mjosi* (Ornithischia, Stegosauria) from the Morrison Formation (Upper Jurassic) of western USA. *PLOS One* 10: e0123503. <https://doi.org/10.1371/journal.pone.0123503>
- Salgado L, Canudo JI, Garrido AC, Moreno-Azanza M, Martínez LCA, Coria RA, Gasca, JM (2017) A new primitive neornithischian dinosaur from the Jurassic of Patagonia with gut contents. *Scientific Reports* 7: 42778. <https://doi.org/10.1038/srep42778>
- Sánchez-Fenollosa S, Escaso F, Cobos A (2025) A new specimen of *Dacentrurus armatus* Owen, 1875 (Ornithischia: Thyreophora) from the Upper Jurassic of Spain and its taxonomic relevance in the European stegosaur diversity. *Zoological Journal of the Linnean Society* 203: zlae074. <https://doi.org/10.1093/zoolinnean/zlae074>
- Sánchez-Fenollosa S, Suñer M, Cobos A (2022) New fossils of stegosaurs from the Upper Jurassic of the Eastern Iberian Peninsula (Spain). *Diversity* 14: 1047. <https://doi.org/10.3390/d14121047>
- Sereno PC (1986) Phylogeny of the bird-hipped dinosaurs (Order Ornithischia). *National Geographic Research* 2: 234–256.
- Sereno PC (1991) *Lesothosaurus*, ‘Fabrosaurids’ and the early evolution of Ornithischia. *Journal of Vertebrate Paleontology* 11: 168–197.
- Sereno PC (1998) A rationale for phylogenetic definitions, with application to the higher-level taxonomy of Dinosauria. *Neues Jahrbuch für Geologie und Paläontologie, Abhandlungen* 210: 41–83.
- Sereno PC (1999) The evolution of dinosaurs. *Science* 284: 2137–2147. <https://doi.org/10.1126/science.284.5423.2137>
- Sereno PC (2005) Stem Archosauria. *TaxonSearch*. <http://taxonsearch.uchicago.edu> [accessed 2 September 2024].
- Sereno PC, Dong Z (1992) The skull of the basal stegosaur *Huayangosaurus taibaii* and cladistic diagnosis of Stegosauria. *Journal of Vertebrate Paleontology* 12: 318–343. <https://doi.org/10.1080/02724634.1992.10011463>
- Siber HJ, Möckli U (2009) The Stegosaur of the Sauriermuseum Aathal. *Sauriermuseum Aathal, Seegräben*.
- Soto-Acuña S, Vargas AO, Kaluza J, Leppe MA, Botelho JF, Palma-Liberona J, Simon-Gutstein C, Fernández RA, Ortiz H, Milla V, Aravena B, Manríquez LME, Alarcón-Muñoz J, Pino JP, Trevisan C, Mansilla H, Hinojosa LF, Muñoz-Walthe V, Rubilar-Rogers D (2021) Bizarre tail weaponry in a transitional ankylosaur from subantarctic Chile. *Nature* 600: 259–263. <https://doi.org/10.1038/s41586-021-04147-1>
- Tanner JB, Dumont ER, Sakai ST, Lundrigan BL, Holekamp KE (2008) Of arcs and vaults: The biomechanics of bone-cracking in spotted hyenas (*Crocuta crocuta*). *Biological Journal of the Linnean Society* 95: 246–255. <https://doi.org/10.1111/j.1095-8312.2008.01052.x>
- Thompson RS, Parish JC, Maidment SCR, Barrett PM (2012) Phylogeny of the ankylosaurian dinosaurs (Ornithischia: Thyreophora). *Journal of Systematic Palaeontology* 10: 301–312. <https://doi.org/10.1080/14772019.2011.569091>
- Thulborn RA (1972) The post-cranial skeleton of the Triassic ornithischian dinosaur *Fabrosaurus australis*. *Palaeontology* 15: 29–60.
- Tumanova TA, Alifanov VR (2018) First Record of Stegosaur (Ornithischia, Dinosauria) from the Aptian – Albian of Mongolia. *Paleontological Journal* 52: 1771–1779. <https://doi.org/10.1134/S0031030118140186>
- Vickaryous MK, Russell AP (2003) A redescription of the skull *Euoplocephalus tutus* (Archosauria: Ornithischia): A foundation for comparative and systematic studies of ankylosaurian dinosaurs. *Zoological Journal of the Linnean Society* 137: 157–186. <https://doi.org/10.1046/j.1096-3642.2003.00045.x>
- Whyte MA, Romano M (2001) Probable stegosaurian dinosaur tracks from the Saltwick Formation (Middle Jurassic) of Yorkshire, England. *Proceedings of the Geologists’ Association* 112: 45–54.
- Wiersma JP, Irmis RB (2018) A new southern Laramidian ankylosaurid, *Akainacephalus johnsoni* gen. et sp. nov., from the upper Campanian Kaiparowits Formation of southern Utah, USA. *PeerJ* 6: e5016. <https://doi.org/10.7717/peerj.5016>
- Xing L, Lockley MG, McCrea RT, Gierliński GD, Buckley LG, Zhang J, Qi L, Jia C (2013) First record of *Deltapodus* tracks from the Early Cretaceous of China. *Cretaceous Research* 42: 55–65. <https://doi.org/10.1016/j.cretres.2013.01.006>
- Xing L, Lockley MG, Zhang J, You H, Klein H, Persons IV WS, Dai H, Dong Z (2016) First Early Jurassic ornithischian and theropod footprint assemblage and a new ichnotaxon *Shenmuichnus wangi* ichnosp. nov. from Yunnan province, southwestern China. *Historical Biology* 28: 721–733. <https://doi.org/10.1080/08912963.2015.1020424>
- Xing L, Lockley MG, Persons IV WS, Klein H, Romilio A, Wang D, Wang M (2021) Stegosaur track assemblage from Xinjiang, China, featuring the smallest known stegosaur record. *Palaios* 36: 68–76. <https://doi.org/10.2110/palo.2020.036>
- Xing L, Niu K, Mallon JC, Miyashita T (2024) A new armored dinosaur with double cheek horns from the early Late Cretaceous of southeastern China. *Vertebrate Anatomy Morphology Palaeontology* 11: 113–132. <https://doi.org/10.18435/vamp29396>
- Yadagiri P, Ayyasami K (1979) A new stegosaurian dinosaur from Upper Cretaceous sediments of South India. *Journal of Geological Society of India* 20: 521–530.
- Yao X, Barrett PM, Yang L, Xu X, Bi S (2022) A new early branching armored dinosaur from the Lower Jurassic of southwestern China. *eLife* 11: e75248. <https://doi.org/10.7554/eLife.75248>
- Zafaty O, Oukassou M, Rigueti F, Company J, Bendrioua S, Tabuce R, Charrière A, & Pereda-Suberbiola X (2024) A new stegosaurian dinosaur (Ornithischia: Thyreophora) with a remarkable dermal armour from the Middle Jurassic of North Africa. *Gondwana Research* 131: 344–362. <https://doi.org/10.1016/j.gr.2024.03.009>
- Zhang J, Xing L, Gierliński GD, Wu F, Tian M, Currie P (2012) First record of dinosaur trackways in Beijing, China. *Chinese Science Bulletin* 57: 144–152. <https://doi.org/10.1360/972011-1963>
- Zhou S (1984) The Middle Jurassic Dinosaurian Fauna from Dashanpu, Zigong, Sichuan. Vol I: Stegosaur. *Sichuan Scientific and Technological Publishing House, Sichuan*, 51 pp. [in Chinese].

## Supplementary Material 1

### File S1

**Authors:** Sánchez-Fenollosa S, Cobos A (2025)

**Data type:** .pdf

**Explanation notes:** 1.1. Institutional abbreviations. — 1.2. Osteological measurements. — 1.3. Operational Taxonomic Unit list. — 1.4. Character list. — 1.5. Additional phylogenetic results. — 1.6. Synapomorphies for major clades. — Supplementary references.

**Copyright notice:** This dataset is made available under the Open Database License (<http://opendatacommons.org/licenses/odbl/1.0>). The Open Database License (ODbL) is a license agreement intended to allow users to freely share, modify, and use this dataset while maintaining this same freedom for others, provided that the original source and author(s) are credited.

**Link:** <https://doi.org/10.3897/vz.74.e146618.suppl1>

## Supplementary Material 2

### Files S2, S3

**Authors:** Sánchez-Fenollosa S, Cobos A (2025)

**Data type:** .zip [.tnt]

**Explanation notes:** **File S2.** Character-taxon matrix (115x30). — **File S3.** Character-taxon matrix (115x31).

**Copyright notice:** This dataset is made available under the Open Database License (<http://opendatacommons.org/licenses/odbl/1.0>). The Open Database License (ODbL) is a license agreement intended to allow users to freely share, modify, and use this dataset while maintaining this same freedom for others, provided that the original source and author(s) are credited.

**Link:** <https://doi.org/10.3897/vz.74.e146618.suppl2>

## Supplementary Material 3

### Files S4–S6

**Authors:** Sánchez-Fenollosa S, Cobos A (2025)

**Data type:** .zip [.txt]

**Explanation notes:** **File S4.** Tree topology in Newick format. — **File S5.** Interval times obtained from the International Chronostratigraphic Chart v2023/09. — **File S6.** FAD and LAD of each OTU.

**Copyright notice:** This dataset is made available under the Open Database License (<http://opendatacommons.org/licenses/odbl/1.0>). The Open Database License (ODbL) is a license agreement intended to allow users to freely share, modify, and use this dataset while maintaining this same freedom for others, provided that the original source and author(s) are credited.

**Link:** <https://doi.org/10.3897/vz.74.e146618.suppl3>